Sigma Journal of Engineering and Natural Sciences
Web page info: https://sigma.yildiz.edu.tr
DOI: 10.14744/sigma.2025.00023

Research Article

Modeling and kinetics investigation of adsorptive properties and regeneration of modified clay on azo dyes removal from aqueous solution using artificial intelligence (ANN, ANFIS) and RSM

Nonso C. OGUANOBI[1,*], Chijioke E. ONU[2], Okechukwu D. ONUKWULI[2], Ephrem N. ANIKE[1], Calistus N. UDE[1]

[1]*Department of Chemical Engineering, Michael Okpara University of Agriculture, P. M. B. Umudike, Abia State, 7267, Nigeria*
[2]*Department of Chemical Engineering, Nnamdi Azikiwe University, P. M. B. Awka, 5025, Nigeria*

ARTICLE INFO

Article history
Received: 05 October 2023
Revised: 25 November 2023
Accepted: 29 December 2023

Keywords:
Adaptive Neuro-Fuzzy Inference Systems (ANFIS); Adsorption; Artificial Neural Network (ANN), Congo Red; Desorption; Optimization; Response Surface Methodology (RSM)

ABSTRACT

Congo red dye (CR) effluent is a toxic waste of environmental concern due to its carcinogenic, mutagenic, and other associated toxicities, its artificial origin, and its complex molecular structure, which make it not easily biodegradable via normal biological wastewater purification methods. In this view, the present work focused on using the adsorption method to completely remove CR from effluent by investigating the adsorptive qualities of acid-modified Ihiala clay (PIC) for CR removal from industrial effluent. The batch system was applied to investigate the influence of process-independent variables with regard to adsorption. The mechanism of adsorption was investigated using intra-particle diffusion, liquid film, and the Boyd model. The thermodynamic properties ΔS, ΔH, ΔG, and Ea were determined. The application of the ANN, ANFIS, and RSM models was to predict the optimum removal efficiency of CR under different variables (temperature, pH, concentration, and contact time) using PIC. The activation resulted in an increase in surface area. Maximum CR removal of 99.3% was observed at pH 2, an adsorbent dosage of 1 g, an adsorbent particle size of 75 µm, an initial dye concentration of 100 mg/l, a contact time of 120 min, and a temperature of 303 k. A maximum adsorption capacity of 127.24 mg/g was obtained. The adsorption mechanism result indicated that the liquid film diffusion process was the rate-limiting step. Thermodynamic results suggested the adsorption process to be endothermic, favorable, spontaneous, and physical. The ANFIS model, with a coefficient of determination of 99.6%, was statistically more significant than the ANN and RSM models. A maximum desorption capacity of 97.5% was achieved after five cycles. Based on the results, PIC is a very reliable and cost-effective alternative adsorbent for CR removal from effluents.

Cite this article as: Oguanobi NC, Onu CE, Onukwuli OD, Anike EN, Ude CN. Modeling and kinetics investigation of adsorptive properties and regeneration of modified clay on azo dyes removal from aqueous solution using artificial intelligence (ANN, ANFIS) and RSM. Sigma J Eng Nat Sci 2025;43(1):316–339.

***Corresponding author.**
*E-mail address: oguanobi.nonso@mouau.edu.ng

This paper was recommended for publication in revised form by Editor-in-Chief Ahmet Selim Dalkilic

INTRODUCTION

Industrial wastewater discharge has increased as a result of industrialization. Industrial wastewater comprises numerous dissolved dyestuffs as well as other pollutants like salts, emulsifiers, leveling agents, dispersing agents, dye bath carriers, and heavy metals [1]. Among all industrial wastewater contaminants, dyes are most stable in aqueous solutions and difficult to deal with due to their artificial origin and their complex molecular structure, which make them not easily biodegradable via normal biological wastewater purification methods. Hence, dye effluent is often purified via chemical and physical techniques like degradation (sonochemical, photochemical, biological, electrochemical) methods [2-6], coagulation and flocculation [7], membrane separation [8], activated carbon adsorption [9], electrochemical removal [10], a fento-biological treatment scheme [8], and oxidation and zonation [11]. However, none of these methods, with the exception of the adsorption process, has efficiently and effectively removed color from waste water [12, 13].Congo red is a synthetic anionic secondary diazo dye or the sodium salt of 3,3'-([1,1'-biphenyl]-4,4'-diyl)bis(4-aminonaphthalene-1-sulfonic acid). CR belongs to the azo dye group derived from benzidine. It's a water-soluble dye that yields a red colloidal solution; its solubility is better in organic solvents such as ethanol. CR has a strong affinity for cellulose fibers, which is why it was first found in the textile industry. However, the use of Congo red in the cellulose industry and other dyeing industries has long been abandoned, primarily because of its carcinogenic, mutagenic, and other associated toxicities and tendency to run and change color when touched by sweaty fingers. CR still finds application in histology to stain tissues for microscopic examination and to serve as an acid-base indicator. The artificial origin, and complex molecular structure of CR, which made it resistant to microbial or bio degradation, together with its other harmful characteristics, necessitate the quest for its total removal from effluent before disposal to the environment.

Adsorption is preferred to other methods because it is an effective, low-cost technique with high treatment efficiency [14, 15]. Of all the tested adsorbents, activated carbon has been the most widely accepted due to its great adsorption capacity. Other low-cost techniques utilizing non-conventional adsorbents are being investigated due to the high running cost of activated carbon adsorption [16, 17]. Some previously explored non-conventional, cost-effective adsorbents were modified biomass [18], Eggplant biomass [19], agriculture waste [20] neem leaf powder [21], black stone cherries [22], hazelnut shell [23], rice hull [24], rattan sawdust [25], garlic peel [26], wheat bran and rice bran [27], jackfruit peel [28], spent brewery grains [29], broad bean peels [30], fly ash [31], and rice husk [32], clay mineral [33, 34, 35], red Clay [36], zeolite-based bio membrane [37], modified clays [38], among others.

Clay's exhibition of high adsorption prowess is a result of its microstructure, which provides highly specific surface areas [39] and the prospect to adsorb polar organic particles and ions on its external surface areas. High adsorption strengths of clay can be further improved through modification [40, 41]. Adsorption and desorption of organic particles on sorbents are controlled primarily by the properties of both the sorbents and the molecules [42]. Natural clays evince negatively charged surfaces and structures, which allow them to adsorb cationic dyes and charged particles at a higher rate than anionic dyes and particles [43]. Most research on the adsorption of CR has focused on studying the influence of factors using the OFAT (one factor at a time method), which is clumpy, dawdling, and cannot appropriately predict the optimum adsorption process parameters. The limits of the OFAT can be solved by using intelligent models in evaluating the adsorption process.

Response surface methodology (RSM) aids in the simultaneous analysis of process parameters that affect a process, even in the presence of complex interactions. It is used to generate a mathematical model capable of determining the optimal operating parameters for a process. It requires a few experimental runs to establish an optimum condition [44, 45]. The artificial neural network (ANN), on the other hand, makes use of biological neurons in processing information. It is used for solving complicated non-linear problems with large data sets. It adequately analyzes complex data sets that are complicated by simple mathematical methods [46]. Adaptive neuro-fuzzy inference systems (ANFIS) are a synergic artificial intelligence model that incorporates the advantages of neural networks and fuzzy logic to create a hybrid model. It can be applied to both non-linear and linear systems with a high degree of accuracy. It is based on the Takagi-Sugeno fuzzy inference system [47, 48]. The objective of this work was to study the adsorptive properties of acid-modified Ihiala clay on the removal of azo dyes (Congo red (CR)) from industrial effluent. Secondly to model an equation for predicting the optimum removal of azo dye (Congo red (CR)) dyes from an aqueous solution using artificial intelligent optimization models (artificial neural network (ANN), and adaptive neuro-fuzzy inference systems (ANFIS)) and response surface methodology (RSM) as well as presenting a comparative study of the studied models. The novelty of the research was the ability to present a comparative study of artificial intelligent models (ANFIS and ANN) and RSM for predicting the optimum point of Congo red dye adsorption on modify Ihiala clay adsorbent.

MATERIALS AND METHODS

The primary raw material used is pure white clay obtained from Uzoakwa village in Ihiala Local Government Area of Anambra State, Nigeria. The secondary raw materials used were HCl (35% purity), H_3PO_4 (85% purity),

NaOH (96% purity), etc. Distilled water was used to prepare the solutions.

Acid Activation of Clay Sample

The clay was dried under the sun for three days to prepare the material for activation. The dried clay sample was crushed to microscale size in a laboratory mortar and pestle, and 75 μm particles were sieved out using dry test sieves. The micro-sized clay sample was contacted with H_3PO_4 in a beaker at a weight-to-volume ratio of 1:5 for 24 hours. The clay slurry was filtered using a separation funnel with Whatman filter paper into residue and filtrate. The obtained residue was washed until a neutral pH of 7 was obtained using distilled water. The washed clay slurry was then oven-dried for four hours at 80 degrees Celsius. The dried activated sample was crushed and sieved again to obtain particle sizes ranging from 75 to 300 μm.

Characterization

The functional group of the activated and raw clay samples was determined by Fourier transform infrared (FTIR) analysis, which was carried out using a Shimadzu Spectrophotometer Model S8400, with samples prepared using the conventional KBr disc method. The adsorbent surface morphologies were determined using a scanning electron microscope (SEM), specifically the Joel Scanning Electron Microscope model JSM 6400.

Batch Adsorption Studies

Batch adsorption was used to investigate the impact of temperature, initial dye concentration, adsorption time, solution pH, adsorbent dosage, and adsorbent particle size on CR uptake on PIC. The stock dye solution was prepared by dissolving a specific amount of dye crystal into a specific volume of distilled water. The solution pH was adjusted using 0.1 N hydrochloric acid (HCl) or sodium hydroxide (NaOH). The dye absorbance was determined with the aid of a UV-visible spectrophotometer. The one factor at a time method (varying one variable while other variables are held constant) was employed in studying adsorbent dosage, particle size, temperature, and pH, while the two factors at a time method was employed for initial dye concentration and adsorption time.

Equilibrium/isotherm and Kinetics Studies

Equilibrium experiments were conducted by contacting specific amount of an adsorbent into glass beakers (250ml) containing a definite volume of different concentrations of CR dye solution of the same pH level. These beakers containing the mixture were placed on shakers (magnetic stirrers) regulated at the fixed temperature level for a period of 150 minutes to ensure equilibrium was attained. Equilibrium dye concentration was determined via a UV-visible spectrophotometer.

Equilibrium dye uptake "q_e (mg/g)" was calculated via expression 1

$$q_e = \frac{(C_o - C_e)V}{m} \quad (1)$$

Percentage removal was calculated via expression 2.

$$\text{Percentage removal (\% Adsorption)} = \frac{(C_o - C_e)}{C_o} \times 100 \quad (2)$$

Where C_e(mg/L) and C_o were equilibrium and initial dye concentrations in solution, V is volume of the solution in liter (L), and m is mass of dry sorbent in gram (g).

Adsorption isotherms are of paramount importance in any adsorption system because they describe the relationship between the adsorbent and the adsorbate. In this research work, four isotherm models were employed: the Langmuir [49], the Freundlich [50], the Vieth–Sladek [51], and the Dubinin–Redushkevich [52], with their expressions in non-linear forms. The parameters of each model provide vital information on the adsorption mechanisms, surface properties, and adsorbent affinity.

Langmuir Adsorption Isotherm

The Langmuir adsorption isotherm is a two-parameter isotherm developed to describe solid-gas-phase adsorption. This empirical model is formulated under the assumption of monolayer adsorption, where the adsorbed layer has a thickness of one molecule. Moreover, it also assumes that adsorption is limited to a restricted number of indistinguishable localized sites and that there is no correlation between the adsorbed molecules, even on adjacent sites. Based on derivation, the Langmuir isotherm relates to homogeneous adsorption as a process with uniform energies of adsorption onto the surface without migration of adsorbate in the plane of the surface (all active sites have identical affection for the adsorbate). The non-linearized form of the Langmuir model can be expressed as follows:

$$q_e = \frac{Q_m K_L C_e}{1 + K_L C_e} \quad (3)$$

Where q_m (mg/g) is Langmuir adsorption capacity constants, K_L (L/mg) is Langmuir energy of adsorption constants, C_e (mg/L) is the equilibrium concentration, q_e (mg g^{-1}) is the amount of dye adsorbed at equilibrium

Freundlich Adsorption Isotherm

The Freundlich adsorption isotherm is a two-parameter isotherm and the foremost known relationship that describes reversible and non-ideal adsorption. Presently, this model is applied to multilayer adsorption, with an uneven distribution of heat from adsorption over the heterogeneous surface. The Freundlich model, in the past designed for adsorption, demonstrated that the adsorbate's ratio to a specific mass of adsorbent to the solute was not constant at varying solution concentrations, and this signifies that the quantity adsorbed is the sum total of adsorption on all sites, with sites of strong binding affinity first

occupied prior to equilibrium or a decrease in adsorption energy. The non-linearized form of the Freundlich model can be expressed as follows:

$$q_e = K_F C_e^{\,1/n_F} \tag{4}$$

Where C_e (mg/L) is the equilibrium concentration, q_e (mg g^{-1}) is the amount of dye adsorbed at equilibrium, K_f is Freundlich adsorption capacity constants and n is the Freundlich adsorption intensity constants, $1/n$ is a measure of the surface heterogeneity

Dubinin-Radushkevich Adsorption Isotherm

The Dubinin-Radushkevich model is a temperature-dependent model, and it predicts the adsorption mechanism. This model was first developed for the sorption of subcritical vapors onto micropore materials by a pore filling mechanism. Typically, it is used to represent the adsorption mechanism on a heterogeneous surface using a Gaussian energy distribution. Despite having unsatisfactory asymptotic properties and failing to predict Henry's law at low pressure, the model has frequently been successful in fitting data on high solute activity and the intermediate range of concentrations. This model was primarily used to differentiate between the chemical and physical sorption of ions through the mean free energy, E per molecule of adsorbate. The non-linearized form of the Dubinin-Radushkevich model can be expressed as follows:

$$q_e = Q_m \exp\left(-b_{DR}\left[RT\, ln\left(1 + \frac{1}{C_e}\right)\right]^2\right) \tag{5}$$

Where q_m (mg/g) is Langmuir adsorption capacity constants, C_e (mg/L) is the equilibrium concentration, q_e (mg g^{-1}) is the amount of dye adsorbed at equilibrium.

Vieth-Sladek Adsorption Isotherm

The Vieth-Sladek isotherm is an empirical model developed to describe, at a constant temperature, the quantity of solute adsorbed onto a solid surface as a function of the concentration of solute in solution. This model was an upgrade to the Langmuir isotherm model, which had limitations in describing multilayer adsorption processes. The Vieth-Sladek isotherm presumes that the sorption process involves a multilayer of solute molecules on the adsorbent surface instead of a monolayer, as in the Langmuir isotherm model. These characteristics make it a valuable instrument for improving and understanding the adsorption process. The model accounts for both the solute concentration in solution and the extent to which the adsorbed molecules cover the solid surface. The non-linearized form of the Vieth-Sladek model can be expressed as follows:

$$q_e = K_{vs} C_e + \frac{Q_m B_{vs} C_e}{1 + B_{vs} C_e} \tag{6}$$

Where q_m (mg/g) is Langmuir adsorption capacity constants, C_e (mg/L) is the equilibrium concentration, q_e (mg g^{-1}) is the amount of dye adsorbed at equilibrium, k_{vs} and B_{vs} are Vieth– Sladek constants.

The same procedures as in an equilibrium experiment were employed in kinetic experiments; the only difference was that the aqueous samples were taken at different time intervals in a kinetic study to determine the uptake of dye at any preset time (t).

Dye uptake at time (t) "q_t (mg/g)" was calculated as follows.

$$q_t = \frac{(C_o - C_t)V}{m} \tag{7}$$

Where C_t is dye concentration at any time (t).

Adsorption kinetics is a very vital aspect of the adsorption system, which sheds light on adsorption mechanisms and dynamics with time. In this research, seven kinetic models were employed: the Elovich [53], pseudo-first order [54], pseudo-nth-order model [55], pseudo-second order [56, 57], intra-particle diffusion [58], liquid film [59], and Boyd models [60]. The liquid film, intra-particle diffusion, and Boyd model were proposed to identify the adsorption mechanism.

Pseudo-first-order Model

The pseudo-first-order model, or Lagergren equation, assumes that the model is applicable over the very initial stage of the sorption process. It also assumes that the degree of change in solute uptake with respect to time is directly proportional to the difference in equilibrium concentration and the quantity of solid uptake with time. Adsorption kinetics follows a pseudo-first-order model when adsorption happens by diffusion via the interface. The non-linearized form of the pseudo-first-order model can be expressed as follows:

$$q_t = q_e[1 - exp(K_1 t)] \tag{8}$$

Where q_e (mg/g) is the amount of adsorbate adsorbed at equilibrium, q_t (mg/g) is the amount of adsorbate adsorbed at time t. K_1 (min^{-1}) is the adsorption rate constants for pseudo-first-order.

Pseudo-second-order Model

The pseudo-second-order kinetic model, an empirical model developed by Ho *et al.*, assumed that the rate-determining step of the adsorption process is purely chemisorption, and this predicts all the adsorption behavior. This aforementioned assumption signifies that the adsorption rate depends more on the adsorption capacity than the adsorbate concentration. This empirical model also forecasts that the rate-determining step of the sorption process should be linked to the covalent forces due to the sharing of electrons between the metal ions and functional groups. The major edge of this empirical model over pseudo-first-order

is its ability to compute directly from the model the equilibrium adsorption capacity, which also puts to an end the theoretical need to determine the adsorption equilibrium capacity by experimentation. The non-linearized form of the pseudo-first-order model can be expressed as follows:

$$q_t = \frac{K_2 q_e^2 t}{1 + K_2 q_e t} \tag{9}$$

Where q_e (mg/g) is the amount of adsorbate adsorbed at equilibrium, q_t (mg/g) is the amount of adsorbate adsorbed at time t, K_2 $gmg^{-1}min$ were the adsorption rate constants pseudo-second-order.

Elovich Model

The Elovich kinetic model assumes that the adsorbent surfaces are energetically heterogeneous and that neither interactions between the adsorbed ions nor desorption could affect the adsorption kinetics significantly at low surface coverage. The major effect of energetic heterogeneity surfaces on sorption equilibrium in gas-solid systems has been proven, while that of liquid-solid systems is yet to be established. The non-linearized form of the pseudo-first-order model can be expressed as follows:

$$q_t = \frac{1}{\beta}\ln(1 + \alpha\beta t) \tag{10}$$

Where q_t (mg/g) is the amount of adsorbate adsorbed at time t, α is the Elovich constant for the initial adsorption rate, and β is the Elovich desorption constant.

Pseudo-nth Order

The pseudo-nth-order kinetic model is an empirical model that seeks to explain the kinetic analysis of order 1 and 2 kinetic parameters. This model will have a substantial effect on the computation of the rate constants since the rate constant is dependent on the reaction order. The non-linearized form of the pseudo-first-order model can be expressed as follows:

$$q_t = q_e - [q_e^{1-n} - (1-n)K_n t]^{1/(1-n)} \tag{11}$$

Where q_e (mg/g) is the amount of adsorbate adsorbed at equilibrium, q_t (mg/g) is the amount of adsorbate adsorbed at time t. K_n ($gmg^{-1}min$) were the adsorption rate constants for pseudo-nth-order; n is the order of reaction.

Adsorption Thermodynamics

Thermodynamics studies the energy changes involved in the adsorption process. Thermodynamic parameters were calculated using the following equations.

$$\Delta G^0 = \Delta H^0 - T\Delta S^0 \tag{12}$$

$$\Delta G^o = -RT\ln K_c \tag{13}$$

Where

$$\text{Where } K_c = \frac{C_s}{C_e} \tag{14}$$

$$\ln K_c = \left(\frac{\Delta S}{R}\right) - \left(\frac{\Delta H}{RT}\right) \tag{15}$$

Where ΔH is the change in enthalpy (heat of reaction), ΔG^o is the standard change in Gibbs free energy and ΔS is the change in entropy. K_c is the equilibrium constant, C_s is the concentration of CR on adsorbent at equilibrium (mg/L), R is general gas constant (8.314J/mol/K), and T is the solution temperature in Kelvin scale.

Activation Energy

The size of activation energy gives insight on the nature of the adsorption i.e., whether the process is chemical or physical. To evaluate adsorption activation energy, Arrhenius rate expression was applied using the equations (16) and (17):

$$K_A = Ae^{-Ea/RT} \tag{16}$$

$$InK_A = InA - \frac{Ea}{RT} \tag{17}$$

Where Ea is the activation energy (KJ/mol) K_A is rate constant of adsorption (g/mg min), R is gas constant, and T is solution temperature in Kelvin (K) [40, 61]. Ea is be obtained from the plot of InK_A against 1/T.

RSM Modeling

RSM uses data obtained from the design of experiments to simultaneously solve multi-variant problems using statistical modeling techniques [44]. A Central composite design (CCD) with five factor levels was used to design the experiment. The factor levels can be assessed in Table S1 of the Supplementary Material.

The process parameters used as independent variables were temperature, pH, concentration, and contact time, while the percentage adsorbed was the response (dependent variable).

The number of experimental data sets in RSM-CCD can be obtained using equation (18) [62].

$$N = 2^n + 2n + n_c \tag{18}$$

Where n stands for the number of input factors, 2^n is the factorial points, 2n is the axial points, and n_c is the center points. The total axial and factorial points were, however, tripled in order to enhance the design's reliability. Ten center points were used. Hence, a total of eighty-two experimental data sets were evaluated. Systematic error was eliminated by carrying out the experiment at random. A second-order polynomial was used to estimate the affinity between the process variables and the response in the equation (19).

$$Y = \beta_o + \sum_{i=1}^{k}\beta_i X_i \ldots\ldots + \ldots\sum_{i=1}^{k}\beta_{ii}X_i^2 \ldots\ldots + \cdots\sum_{i=1}^{k-1}\sum_{j=1}^{k}\beta_{ij}X_iX_j \tag{19}$$

where Y is the calculated response; β_i, β_{ii}, and β_{ij} are the coefficients calculated from the second-order polynomial equation for the linear, pure quadratic, and cross products of X_i, X_i^2 and $X_i X_j$, respectively, while β_o is the model constant. Design expert software version 13 was used in the design and analysis of the RSM-CCD.

ANN Modeling

The neural network toolbox of MATLAB R2015 (The Mathworks Inc.) was utilized in modeling and analyzing the prediction of the percentage of CR dye adsorbed using an artificial neural network (ANN). ANN is inspired by biological neurons, where the weighted inputs that arrive at each neuron are passed through a nonlinear activation function to produce an output signal [63].

For adequate modeling of the ANN process, the eighty-two data sets used in the RSM-CCD were tripled and used in the ANN. Hence, two hundred and forty-six data sets were used in the ANN. The data sets were divided into three categories: training, testing, and validation, with 70%, 15%, and 15%, respectively, allocated to each randomly. The ANN architecture consists of input nodes (four input parameters), hidden neuron layers, and an output node (the response). The ANN architecture is given in the Supplementary Material.

The optimum number of hidden layers was obtained by iteration to avoid over-fitting and a reduction in the convergence rate [64]. Minimum mean square error (MSE) and maximum correlation coefficient (R^2) were the parameters involved. Multi-Layer Perceptron (MPL), which made use of back propagation, was the learning algorithm used for the modeling. To regularize the bias value, trainlm was used as the training function. To reduce network error, the process parameters and response were normalized between 0 and 1 [65]. The process parameters and the response were normalized between 0 and 1 to reduce network error [65].

ANFIS Modeling

The fuzzy logic toolbox of MATLAB R2015 (The Mathworks Inc.) was used in ANFIS modeling and prediction of optimal CR dye adsorbed. Using the fuzzy inference system (FIS) principle, the ANFIS is modeled as a five-layered network, as shown in Fig. S2 of the Supplementary Material. The first layer accepts the process variables (temperature, pH, concentration, and contact time) as inputs to the fuzzy system network. The second layer node decides the fuzzy rules, which it relays to the third layer for normalization of the activity rules

The fourth layer adopts the nodes and converges the parameters, which it sends to the fifth layer as a single output layer (percentage of CR adsorbed) [66]. The same two hundred and forty-six data sets used in ANN modeling were utilized in ANFIS modeling. A hybrid method of optimization was used with zero error tolerance.

Comparative Analysis of RSM, ANN, and ANFIS Models

The predicted percentage removal of CR by RSM, ANN, and ANFIS was compared to the experimental values and subjected to statistical error indices. Five statistical error functions were used. They were used to investigate the accuracy of the models in predicting the removal of CR from wastewater by the adsorption process. The significance of the model was based on smaller values of the root mean square error (RMSE), average relative error (ARE), sum of squared errors (SSE), hybrid fractional error function (HYBRID), and a higher value of the correlation coefficient (R^2).

Adsorbent Recycling/ Regeneration

Recycling is the method of processing materials that would have otherwise been thrown away as trash into new products, which minimizes production costs as well. This phenomenon in the adsorption process is termed desorption. Desorption is simply using an eluent to create sorption equilibrium or destabilize the bond between the pollutant (bulk phase) and the adsorbing surface. Different desorption methods, including chemical regeneration, thermal regeneration, thermochemical regeneration, steam regeneration, bio-regeneration, vacuum regeneration, electrochemical regeneration, pressure swing regeneration, ozone regeneration, microwave regeneration, oxidative regeneration, and ultrasound regeneration, have been used in the regeneration or recycling of adsorbents. In this research, a chemical regeneration method was employed, and the eluents used were HCl and propanone (acetone). The use of HCl was because the pollutant to be desorbing is cationic, and therefore HCl destabilized or broke the intermolecular bond (van der Waals forces) between the pollutant (bulk phase) and the adsorbing surface, leading to adsorption, while Propanone was used because of its property to dissolve other substances without destroying their structure.

Batch Desorption

Exhausted adsorbent was mixed with the eluent and stirred at a specific temperature for 30 minutes per cycle until equilibrium was reached. It was then filtered into filtrate and residue adsorbent at the end of each cycle. The filtrate was for dye analysis using a UV spectrophoto2wmeter for desorption efficacy, while the residue sorbent was washed with water to remove the eluting agent, which was then oven dried and kept for reuse in a fresh process. The amount (quantity) in mg/g and efficacy in % of desorbed adsorbate (pollutant) were calculated using equations (20) and (21), respectively.

$$\text{Amount /quantity desorbed (mg/g)} = A_{des} = \frac{C_s * V}{M} \quad (20)$$

$$\text{Efficiency of desorbed (\%)} = \%_{des} = \frac{A_{des}}{C_{ad}} X\ 100 \quad (21)$$

Where, C_s is concentration of adsorbate desorbed in mg/g, C_{ad} is concentration of adsorbate adsorbed in mg/g,

M is weight of exhausted adsorbent in gram and V is volume of the eluent in liter.

RESULTS AND DISCUSSION

Adsorbent Characterization

FTIR analysis

The FTIR spectra of the raw Ihiala clay and the acid-modified Ihiala clay are given in Figures 1a and 1b, respectively. Comparing the figures, a higher number of peaks was observed in Fig. 1b, and this is as a result of the acid modification that removed impurities contained in the raw clay material. The peaks observed in Fig. 1b are composed of various functional groups that are responsible for the binding of CR dye, and they are amide, alkane, alcohol, and alkyne halide.

SEM micrographs

The scanning electron micrographs (SEM) of the raw Ihiala clay and the acid-modified Ihiala clay are shown in Figures 2a and 2b. Figure 2b displayed a greater number of heterogeneous layers of pores and the internal surface of the

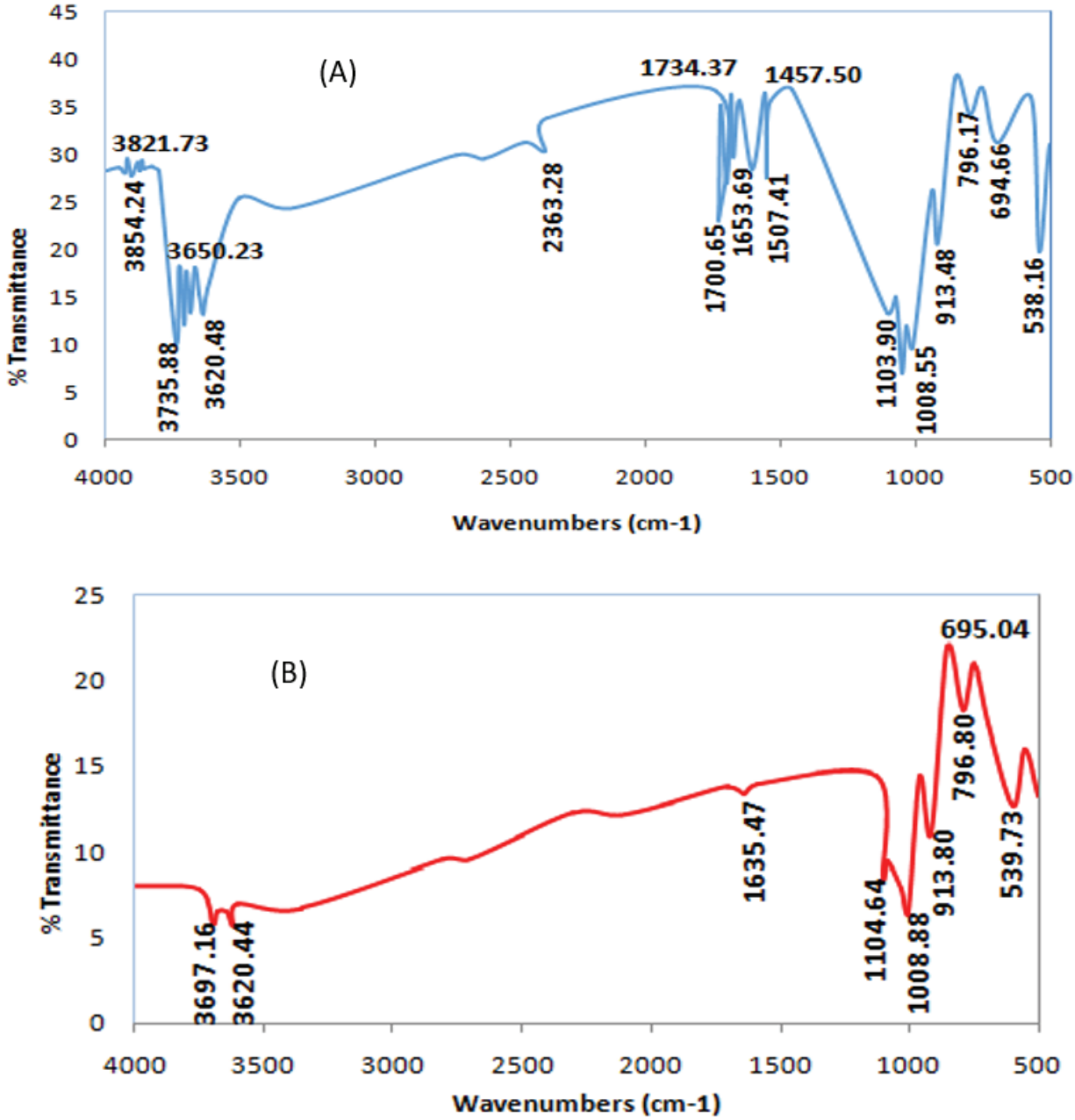

Figure 1. FTIR spectra of (a) raw Ihiala clay and (b) of acid activated Ihiala clay.

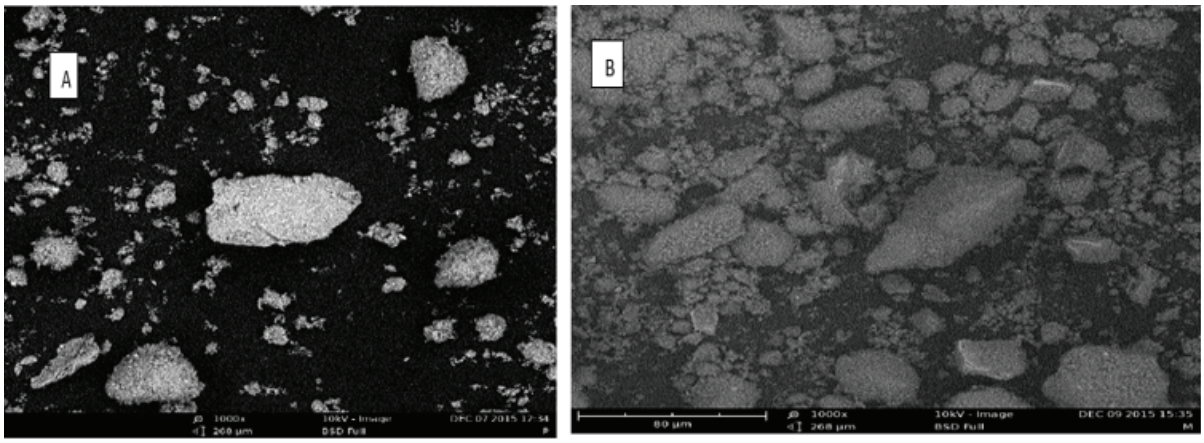

Figure 2. SEM Micrograph of the clay (2a) before activation and (2b) after activation.

clay material than Figure 2a. This observed development is a result of the modification that exposed the interior and inner surface of the clay sample to the acid particles. This increased the pores of the adsorbent, thereby making it a good adsorbent.

Effects of Process Variables on CR Adsorption

Effect of adsorbent particle size

The effect of sorbent particle size was studied at particle size ranges of 75, 150, 300, 650, and 850 μm at a constant temperature of 303 k, an adsorbent dosage of 1 g, initial dye concentration of 100 mg/l, a time of 60 min, and a pH of 2. The result of the study, as reported graphically in Fig. 3a, shows that the percentage dye uptake decreased with sorbent increases in particle size, from 72.3% at 75 μm to 44.6% at 850 μm. This outcome proved that large particles produce a less heterogeneous layer of pores and surface area. Moreover, the disintegration of large particles opened channels and tiny cracks on the adsorbent surface and thereby increased the availability of pores for better adsorption and diffusion. The result of this study concurs with the previous work, which reported that an increase in adsorbent particle size distinctly decreased the amount of dye adsorption as well as the percentage of dye removed [67]. El-Halwany (2010) also reported that dye removal increased with the decrease in particle size [24].

Effect of adsorbent dosage

Adsorbent dosage effect was investigated for the dosage range of 0.2, 0.4, 0.6, 0.8, and 1 g/100 ml of CR at a constant temperature of 303 k, an adsorbent particle size of 150 μm, an initial dye concentration of 100 mg/l, a time of 60 min, and a pH of 2. The result of the study, as reported graphically in Fig. 3b, shows that the percentage of adsorption increased with an increase in adsorbent dosage, from 45.4% at 0.2 g to 83.5% at 1 g. This significant increase in dye adsorption per increase in adsorbent dosage is due to an increase in the surface area of active functional groups, which also increased the availability of adsorption sites [68]. The result also showed a notable decrease in quantity adsorbed per unit mass of adsorbent with an increase in dosage. This decrease in unit adsorption as dosage increases is due to adsorbent sites remaining unsaturated during the adsorption reaction. The result of this study is in agreement with the previous works, which reported that an increase in Fe-Bent dosage distinctly decreased the amount of arsenic in solution [69, 70].

Effect of concentration and contact time

The effect of initial dye concentration was studied at concentration ranges of 100, 200, 300, 400, and 500 mg L^{-1} per 1 g adsorbent dosage at a contact time range of 2–150 minutes at a constant temperature of 323 k, an adsorbent particle size of 75 μm, and pH 2. The result as reported in Fig. 3c shows that as the rate of CR adsorbed per unit mass increased with an increase in initial ion concentration, the adsorption percentage decreased. This may be due to the low ratio of the initial number of dye molecules to the available surface area at a lower concentration. Furthermore, the result also revealed an increase in quantity of adsorption with increasing contact time at all concentrations until equilibrium was reached after 90 minutes. This is a result of the driving force supplied by the initial dye concentration to conquer the resistance to the mass transfer of dye between the solid phase and liquid phase. Finally, the result also showed that the process followed three-step processes: rapid initial adsorption (bulk diffusion), a period of slower uptake (pore diffusion and intra-particle diffusion), and a period of no significant uptake (equilibrium stage). The findings are consistent with previous work, which reported that at higher concentrations of As(V), adsorption efficiency decreased due to a decrease in available active sites [70]. Mahmoud et al. (2019) also reported that the equilibrium of the PNP adsorption on the montmorillonite clay was reached after 120 min [71].

Effect of pH

The effect of pH is essential when the adsorbing molecules can ionize in response to pH. CR is a diazo/anionic dye and maintains its red color at pH 5, while below pH 2, the solution changes from red to dark blue, at pH 3, it changes to blue-violet, and the original red color is different above pH 10. The effect of pH is studied between the pH ranges of 2 and 12, at a constant temperature of 303 k, an adsorbent particle size of 150 µm, an initial dye concentration of 100 mg/l, a time of 60 min, and an adsorbent dosage of 0.8 g. The result of the study, as reported graphically in Fig. 3d, shows that the highest removal efficiency of 82.2% was achieved at pH 2, whereas the highest removal efficiency of 72.8% occurred at pH 4. This disparity at positive pH is a result of the relatively low solubility of the CR ion at pH less than 2. The H^+ ion concentration in a system is relatively high at a low pH level, and the adsorbent surface acquires a positive charge by adsorbing H^+ ions. As the clay surface becomes positively charged by adsorbing H^+ ions at low pH, a significantly strong electrostatic attraction appears between the positively charged sites. A negatively charged surface site on the clay does not favor the adsorption of anionic CR molecules due to the electrostatic repulsion. Furthermore, the low CR adsorption at an alkaline pH is a result of adsorption site competition between the CR dye molecule and excess OH-ions. A subsequent increase at pH 10, which declines thereafter, may be due to the hydrolysis or liquefaction of adsorbent surfaces, which create positive charged sites. Based on the obtained result, it can be concluded that the removal of Congo red dye from aqueous solutions using PIC is pH-dependent. This study's findings are consistent with previous works which reported that pH 2 was optimal for removing Congo red using CHCFe and Indian Jujube Seeds (IJS) (Zizyphus maruritiana) [72, 73, 74]. Popoola et al. (2021) and Lafi et al. (2019) also reported optimum pH 3 for the removal of Congo red using synthesised coal graphene and activated coffee waste [75, 76]. Moreover, Mahmoud et al. (2019) reported that the PNP adsorption on montmorillonite is pH-dependent [71].

Effect of temperature

Temperature as a process variable determines the nature of adsorption, whether it's an endothermic or exothermic system. The impact of temperature on CR uptake

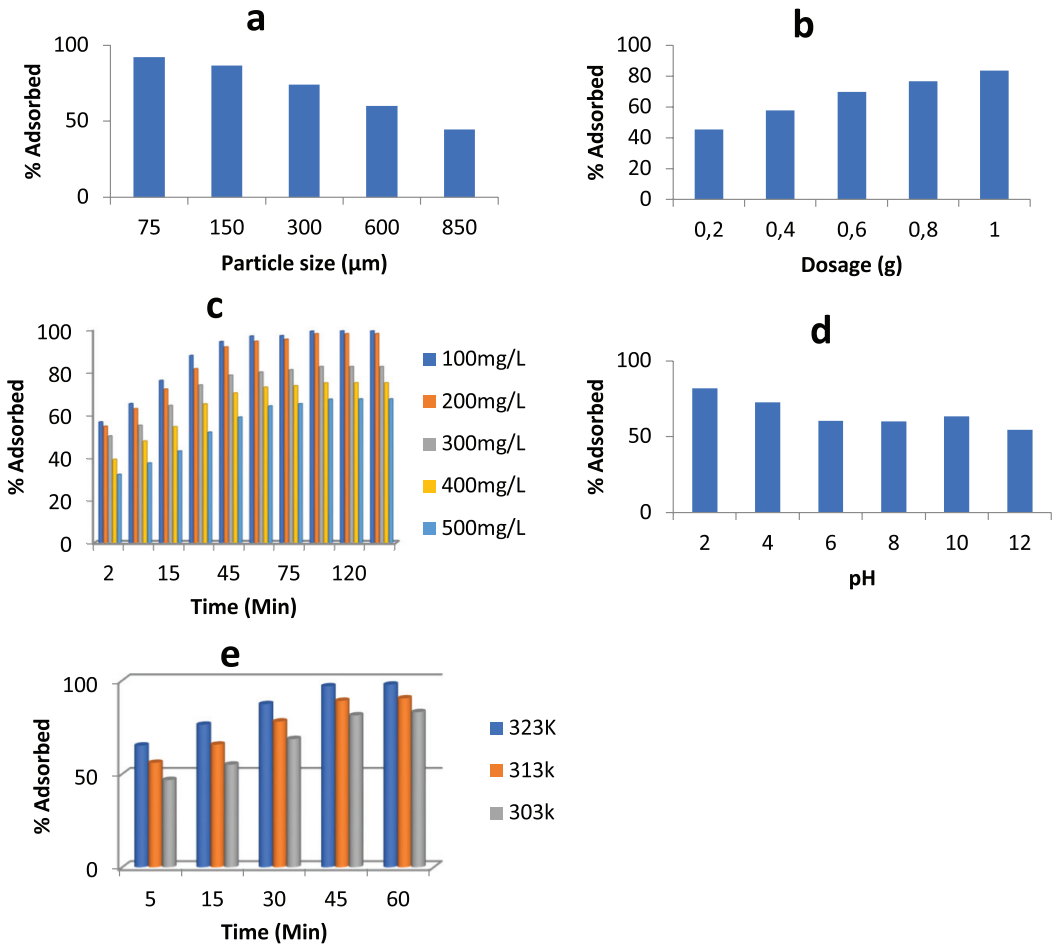

Figure 3. Effects of process variables showing influence of (a) particle size, (b) dosage, (c) concentration, (d) pH, and (e) temperature on the percentage of CR adsorbed.

was examined using a temperature range of 303K, 313K, and 323K at a constant adsorbent dosage of 1g, an adsorbent particle size of 75 μm, an initial dye concentration of 100 mg/l, a time period of 60 min, and pH 2. The result of the study, as reported graphically in Fig. 3e, shows that an increase in the amount of CR uptake from 83.1% at 303K to 97.8% at 323K as the temperature of the solution increased was observed; this phenomenon certifies the adsorption of CR on PIC as an endothermic system. The increase in amount of CR uptake as the temperature of the solution increases is a result of an increase in the mobility of dye molecules; furthermore, a rise in temperature could also cause the adsorbent's internal structure to swell or enlarge, which enables large molecules of dye to penetrate further. Based on the results obtained, it is possible to conclude that the removal of Congo red dye using PIC is temperature-dependent. The result obtained is in harmony with the previous work on PNP adsorption on montmorillonite, which reported that adsorption was more energetically favorable to occur at higher temperatures [71]. Oguanobi et al. (2019), Mahmoodi et al. (2011), and Salleh et al. (2011) also reported similar results of the same trend [40, 77, 78]. Finally, based on the achieved results of process variables, it is clear that the removal of Congo red dye using PIC is dependent on temperature, initial dye concentration, pH of solution, adsorbent particle size, contact time, and adsorbent dosage.

Nonlinear Equilibrium Modeling

The equilibrium adsorption study studies the affinity between the amounts of CR dye molecule adsorbed per unit mass of sorbent and the fluid-phase equilibrium concentration in bulk solution at a constant temperature [79]. The non-linear expression of the Langmuir, Dubinin-Radushkevich, Vieth-Sladek, and Freundlich models was used to analyze equilibrium results. The details of their non-linear form are shown in Section 2.4 and in the graph of Figure 4. The respective constants of each model and statistical analysis were evaluated using software and tabulated in Table 1.

The Langmuir theory presumes that adsorption occurred at the adsorbent surface while saturation took place when equilibrium was attained, which is to say the adsorbent site must have been filled with dye molecules to the extent that adsorption cannot occur at that site again. The model's critical feature is expressed by an equilibrium parameter R_L, which is a dimensionless constant or separation factor. R_L is calculated using the expression from equation 22.

$$R_L = \frac{1}{1 + K_L C_o} \tag{22}$$

The R_L value reflects the nature of adsorption. An adsorption system is considered unfavorable if $R_L>1$, Linear if $R_L=1$, favorable if $0<R_L<1$, and irreversible if $R_L=0$. The Langmuir equilibrium parameter and constant R_L, K_L, and Q_m values were listed in Table 1, and from the table, R_L = 0.59 is greater than zero and less than one, thereby certifying favorable adsorption of CR dye. The K_L relates to the heat of adsorption, and a positive value for the K_L signified that the affinity of the active sites for CR was improved with temperature, and this outcome validated the effect of temperature, which reported an increase in the amount of CR uptake as the temperature of the solution increased. In addition, Langmuir yields the highest value of maximum adsorption capacity (Q_m) compared to the Vieth-Sladek and D-R models.

The Freundlich equation is an empirical relationship between the quantity of gas adsorbed into a solid surface and the gas pressure. It is applicable to adsorption processes that occur on heterogeneous surfaces. Freundlich isotherm constant n_f studies adsorption intensity (the favorability of the adsorption process). Favorable and physical adsorption is obtained when the n_f value is within the range of $1<n_f<10$, and any value outside this range may be a linear or chemical process. The constant studies the uptake capacity, whose reasonable value signifies a higher uptake capacity. From Table 1, the n_f value fell within the range of $1<n_f<10$ and thereby certified the uptake of CR dye on PIC a favorable and physical process. The value of $1/n$ measures the surface heterogeneity and distribution of site energies with ranges between 0 and 1. A system seems more heterogeneous when $1/n$ value approaches zero. The value of $1/n$ ranging between 0.1 and 0.5 is indicative of favorable adsorption, while the value between 0.5 and 1.0

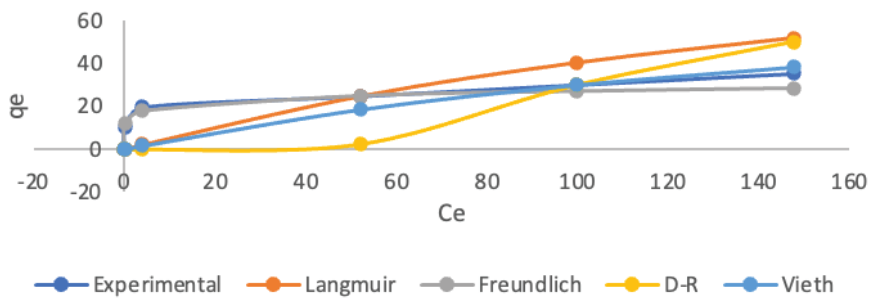

Figure 4. Non-linear isotherm plot.

indicates easy adsorption of ions; otherwise, if $1/n > 1$, it signifies difficult adsorption of ions. From Table 1, the $1/n$ value fell within the range of $0<1/n< 0.5$ and thereby certified the uptake of CR dye on PIC a favorable process and this outcome validates the n_f result.

The Vieth–Sladek isotherm is used for estimating diffusion rates in solid materials from transient adsorption. The Vieth-Sladek constant values for the non-linear model are listed in Table 1. The Dubinin-Radushkevich (D-R) isotherm is a temperature-dependent model, and it predicts the adsorption mechanism, i.e., whether the process of the adsorption is a physical or chemical adsorption process. The feature of the D-R model is being evaluated through the mean free energy "E" value in KJ mol^{-1}. The D-R isotherm constant b_{DR} relates to the mean free energy of adsorption through the expression of Equation 23 [80].

$$E = \frac{1}{\sqrt{2b_{DR}}} \quad (23)$$

An adsorption process is physical if the "E" value falls below 8KJ mol^{-1} and chemical if the "E" value falls within the range of 8–16Kj mol^{-1} [81, 82, and 83]. The "E" value below 8 KJ mol^{-1} signifies that the metal ion sorption process was of weak ion exchange while the "E" value within the range of 8–16 Kj mol^{-1} signifies that the metal ion sorption process was of strong ion exchange. From Table 1, the "E" value as seen fell below the range of 8 KJ mol^{-1}, thereby confirming the uptake process of CR dye as a physical adsorption process and this signifies a weak adsorbate-adsorbent relationship, which might result in the desorption of the adsorbed ions after equilibrium is reached.

Nonlinear Kinetic Modeling

Adsorption kinetics is a phenomenon in water treatment as it represents the adsorbate uptake rate at the solid-solution interface with respect to time. For evaluation of the adsorption kinetics of CR onto PIC, the pseudo-first-order, pseudo-second-order, Elovich, and pseudo-nth-order models were employed to fit the experimental data. The details of their non-linear form are shown in Section 2.4 and in the graph of Figure 5.

From Table 1, it can be seen that the parameter "n" of the pseudo-nth-order kinetic model is 2.0017, which signifies that the adsorption of CR on PIC was governed by reaction order 2. This outcome validates the statistical analysis result of the error function, which predicts the pseudo-second-order model as the best-fit kinetic model to describe the process. The calculated adsorption capacity ($q_e cal$) values of pseudo-first-order, pseudo-nth-order, and pseudo-second-order, as also reported in Table 1, fell within the range of plus or minus 1 to that of the experimental adsorption capacity value (($q_e exp$); this also validates the accuracy of the software prediction. Additionally, the pseudo-second-order, pseudo-first-order, and pseudo-nth-order values for parameters K_2, K_1, and K_n were all significant.

Moreover, the Elovich parameter "β" is the desorption constant, which specifies the nature of the process, i.e., if the process is reversible or irreversible [84]. The positive value of the constant indicated that the adsorption of CR onto PIC was reversible, and this validated the Langmuir parameter value of R_L which also predicted the system to be a reversible process. The significant values for parameter "ho" of pseudo-second-order and pseudo-first-order, as

Table 1. Isotherm and Kinetic model calculated parameters for the adsorption of CR on PIC

Isotherm model	Parameter	Value	Kinetic model	Parameters	Value
Langmiur	Q_m	127.24	**Pseudo-First order**	qe cal	9.59
	K_L	0.0046		K_1	0.1062
	R_L	0.594		ho	1.0179
	ARE	0.069		X^2	0.0073
Freundlich	K_F	14.96	**Pseudo-Second order**	qe cal	10.27
	n_F	7.84		K_2	0.0188
	1/ n_F	0.1275		ho	1.9863
	ARE	1.57		X^2	0.0061
Vieth-Sladek	K_{vs}	0.0009999	**Pseudo nth-order**	qe cal	9.27
	Q_m	89.74		K_n	0.0582
	B_{vs}	0.004999		n	2.0765
	ARE	5.16		X^2	0.0725
	Q_m	77.1698			
Dubinin-Redushkevich	b_{DR}	0.001323	**Elovich**	β	0.4014
	E	0.019		α	3.3951
	ARE	6.2033		X^2	0.1357

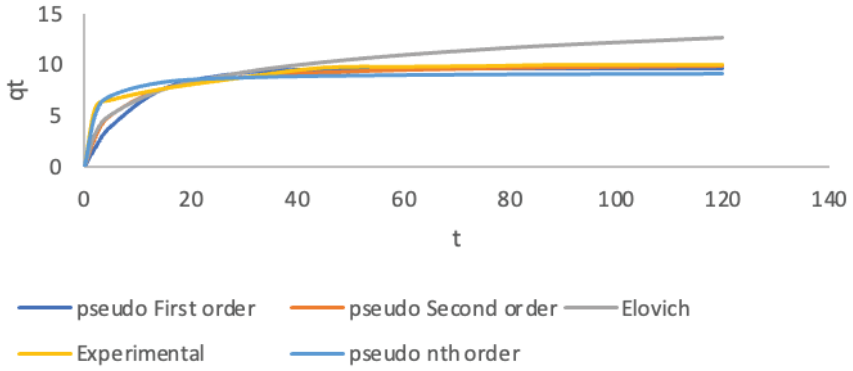

Figure 5. Non-linear kinetics plots

well as the α value of Elovich, indicate bulk diffusion at the initial adsorption stage.

Statistical Analysis

The goodness-of-fit model prediction of the experimental data via equilibrium and kinetics models for the uptake of CR dye on PIC was evaluated using non-linear error functions such as the average relative error (ARE) for equilibrium models and the chi-square test (X^2) for kinetic models. The best of the error parameters is based on the idea that the smaller the value of the error parameter, the better the fit. The obtained results of the error parameters for both equilibrium and kinetics studied models are tabulated in Table 1. From the result, the Langmuir model with the lowest value of the error parameter (ARE) best describes the equilibrium uptake of CR dye on PIC, while the pseudo-second-order model with the smallest value of the error function chi-square test (X^2) best describes the kinetic uptake of CR dye on PIC. Finally, from the achieved results of equilibrium and kinetic modeling, it can be deduced that all the studied models follow the adsorption process, irrespective of the Langmuir model, and pseudo-second order has been the best.

Adsorption Mechanism

Weber and Morris (1963) proposed the intra-particle diffusion model to forecast the rate-control step and identify the diffusion mechanism [58]. This model involves three steps: the boundary layer diffusion or external surface adsorption; the intra-particle diffusion, i.e., the gradual stage of adsorption; and the equilibrium stage, i.e., the point at which the intra-particle diffusion slows down as a result of a very low concentration of dye in the solution. According to this hypothesis, intra-particle diffusion becomes the rate-controlling step if the graph of qt versus $t^{1/2}$ in mg/g is linear and passes through the origin, but if the data show multi-linear plots, then two or more steps influence the sorption process. The boundary layer thickness is indicated by the constant or intercept value of the linear plot of qt vs $t^{1/2}$ (mg g-1), and the higher the intercept, the more significant the influence of the boundary layer [85]. The expression of the Intra-particle model can be expressed as follows:

$$q_t = K_{id}\sqrt{t} \tag{24}$$

Where q_t (mg/g) is the amount of adsorbate adsorbed at time t, and k_{id} ($mgg^{-1}min^{1/2}$) is the intraparticle constant obtained from the slope of q_t versus $t^{1/2}$.

Figure 6a shows multi-linear plots with high intercept values, indicating that the sorption process is influenced by two or more steps. Additionally, the high intercept value denotes a stronger impact of the boundary layer on the process. The results confirm that the adsorption was somewhat controlled by boundary layer diffusion (external surface adsorption) [86].

Liquid film diffusion model

The liquid films model assumes that the contact between the liquid films of the sorbate and sorbent could be a determining force in adsorption. This contact between the sorbent and adsorbate caused the movement of the dye ion from the bulk solution to the liquid film surface. The diffusion impediment exerted determines the degree of involvement of film diffusion. Therefore, the degree of adsorption can be determined by external diffusion, internal diffusion, or both. Internal diffusion regulates the movement of solute materials from the adsorbate surface to the internal surface of the adsorbent. The liquid film model can be expressed as follows:

$$-\ln 1 - F = -K_{fd}t \tag{25}$$

Where F is the fraction of solute adsorbed at equilibrium and F value can be evaluated using

$$F = \frac{q_t}{q_e} \tag{26}$$

Where q_t and q_e are the amount dye adsorbed on the adsorbent at any time t and at equilibrium respectively.

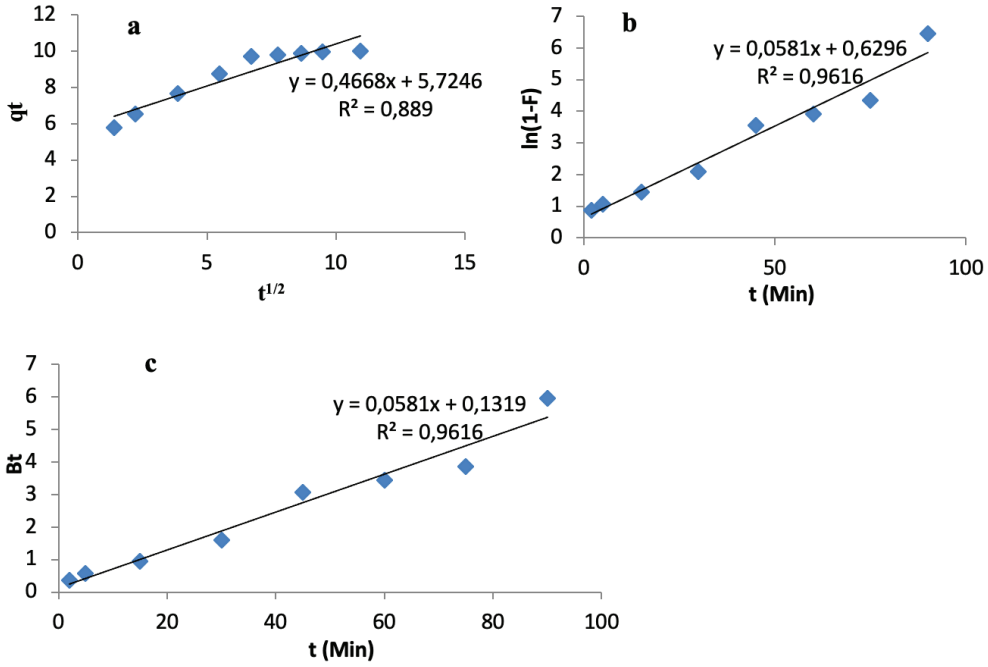

Figure 6. Adsorption mechanism plots for (a) Intra-particle diffusion model, (b) Liquid film model, and (c) Boyd diffusion model.

A plot of — ln (1—F) versus t gives a liquid film plot, and the liquid film diffusion constant K_{fd} is obtained from the slope of — ln (1—F) versus t. The liquid film model assumes that a linear plot of — ln (1—F) versus time with no intercept would indicate that intra-particle diffusion through the liquid surrounding the solid sorbent regulated the sorption process kinetics, but if the plot is nonlinear or linear but does not pass through the origin, liquid film diffusion (external mass transport) becomes the rate-limiting step in the uptake of Congo red dye onto PIC.

Figure 6b shows a non-zero intercept, which highlights the significance of liquid film diffusion as the rate-determining step and the kinetics of the adsorption process as being probably diffusion-limited [85]. The fact that the liquid film diffusion regression coefficient (R^2) value of 0.9616 is significantly greater than the intra-particle diffusion (R^2) of 0.889 indicates the significance of film diffusion as a rate-determining step in the adsorption process. Additionally, the obtained low value of liquid film diffusion constant (K_{fd}) of 0.0581 compared to 0.4668 of the intra-particle rate constant (k_{id}), validates the prediction of the intercept and R^2 values, which establish liquid film diffusion as the rate-limiting step during the sorption of CR on PIC.

Boyd model

The Boyd model is an empirical equation that gives insight into the adsorption kinetic mechanism. This model is applied to determine the slow step involved in the adsorption process, or the rate-determining step for an adsorbent. The Boyd model can be expressed as follows:

$$F = 1 - \left(\frac{6}{\pi^2}\right) exp^{(-Bt)} \tag{27}$$

$$Bt = -0.4977 - \ln(1 - F) \tag{28}$$

Where Bt is the function of F and F is the fraction of solute adsorbed at different times, t. The Bt values at different contact times, t, can be evaluated using equation 28 in the case of $F > 0.85$. The F value can be calculated using equation 26.

$$F = \frac{q_t}{q_e} \tag{26}$$

Where q_t and q_e are the amount dye adsorbed on the adsorbent at any time t and at equilibrium respectively.

The Boyd model plot is obtained by plotting Bt values against time, and the model proposes that if the plot of Bt against t is linear and passes through the origin, it is the pore diffusion or particle diffusion mechanism that controls the rate of mass transfer; if the plot is nonlinear or linear but does not pass through the origin, film diffusion (external mass transport) dominates the rate of mass transfer [87].

Figure 6c shows that the Boyd plot is linear but did not pass through the origin, which signifies that intra-particle diffusion was not the sole control process for the adsorption of CR dye ions on PIC. This result is in harmony with the intra-particle diffusion and liquid film model results,

which establish the kinetic adsorption of CR dye on PIC as a film-diffusion mechanism system. Finally, based on all the achieved adsorption mechanism results, it can be deduced that the liquid film diffusion process was the rate-limiting step in the uptake of Congo red dye onto PIC.

Thermodynamics and Activation Energy

The thermodynamic parameters ΔG^o, ΔH^o, and ΔS^o were used to explain the fluctuation in dye adsorption efficiency with respect to temperature [88]. The thermodynamic and activation energy plots can be seen in Figs.S3 and S4 of the Supplementary Material.

The slope of the plots is equal to $\Delta H^o/R$ and its intercept is equal to $\Delta S^o/R$. The calculated parameters of ΔG, ΔH, and ΔS are shown in Table 3.

The obtained negative values of the Gibbs free energy (ΔG) indicate the spontaneous nature of the adsorption, while the positive value of ΔS indicates increased randomness at the solution or solid interface and an increase in the degree of freedom of the adsorbed species [89]. Thus, the adsorption of CR was favored on the adsorbent. Reddy et al. (2011), reported similar results of the same trend [74].

The magnitude of the activation energy gives insight on whether the adsorption process is primarily chemical or physical. The activation energy of the physisorption process was typically 5 to 40 kJ/mol, whereas the activation energy of chemisorption was 40 to 800 kJ/mol [90]. To determine the adsorption activation energy, Arrhenius theory was utilized using the expression of Equation 17.

It is clearly observed from Table 2 that the E_a value for CR adsorption on PIC is positive and below 40 kJ/mol, which indicates that the adsorption of CR using PIC is feasible and a physisorption process. The result is in harmony with the Freundlich constant "n_f" and E value of the D-R result, which also concludes the uptake of CR on PIC, a physical process. Finally, based on the achieved thermodynamic results, it can be deduced from the decrease in Gibbs free energy as the temperature increases that the uptake of Congo red dye onto PIC is more likely to happen at higher temperatures, thereby suggesting an endothermic process.

Table 2. Thermodynamics parameters for the adsorption of CR on PIC

Temp (K)	$K_c = \frac{C_S}{C_e}$	ΔG (KJ/mol)	ΔS (KJ/mol)	ΔH (KJ/mol)	E_a (KJ/mol)
303	**4.9205**	**-4.0140**			
313	**9.4790**	**-5.8527**	**0.3064**	**89.2175**	**6.9762**
323	**44.5498**	**-10.1955**			

Table 3. ANOVA and model coefficients for CR adsorption

Source	Sum of squares	Df	Mean squares	F-value	p-value Prob>F
Model	1276.27	14	91.16	94.31	< 0.0001
A-pH	17.36	1	17.36	17.96	< 0.0001
B-Temperature	17.28	1	17.28	17.88	< 0.0001
C-Concentration	721.13	1	721.13	746.04	< 0.0001
D-Contact time	70.21	1	70.21	72.64	< 0.0001
AB	18.68	1	18.68	19.32	< 0.0001
AC	34.17	1	34.17	35.35	< 0.0001
AD	5.62	1	5.62	5.81	0.0187
BC	3.70	1	3.70	3.82	0.0547
BD	0.34	1	0.34	0.35	0.5551
CD	188.02	1	188.02	194.52	< 0.0001
A^2	3.39	1	3.39	3.51	0.0655
B^2	20.66	1	20.66	21.37	< 0.0001
C^2	49.79	1	49.79	51.51	< 0.0001
D^2	68.12	1	68.12	70.47	< 0.0001
Residual	64.76	67	0.97		
Lack of fit	59.47	10	5.95	63.99	< 0.0001
Pure error	5.30	57	0.093		
Cor total	1341.03	81			

A similar phenomenon was reported for PNP adsorption on montmorillonite [71] and for the adsorption of basic dye using acid-treated Kenal fiber char [89].

RSM Modeling

Design expert was used to analyze the result. The summary of the P-value and the model summary statistics are presented in Table S2 of the Supplementary Material.

The quadratic model for optimum point prediction of the process was suggested from the CCD model with high adjusted and predicted R-squared values of 0.9416 and 0.9255, respectively. The correlation coefficient was 0.9517 for the quadratic model. Table 3 presents the analysis of variance (ANOVA) and confirms the adequacy of the quadratic model.

Significant terms of the model were checked using F-values and P-values. The higher the F-value, the smaller the P-value, and the more significant the corresponding coefficient. The higher model F-value of 94.31 implied that the model was significant, and P-values whose coefficients were less than 0.05 became the significant terms; therefore, A, B, C, D, AB, AC, AD, CD, B^2, C^2, and D^2 were significant terms. A similar phenomenon was reported by Amini et al. 2008 and Kim et al. 2003 [91, 92]. The empirical correlation between the variables (response and independent) in the coded form on the basis of experimental results was reported in Equation 29.

$$Y_{PIC}\,(\%) = +97.74 - 0.54A + 0.54B - 3.47C - 1.08D - 0.62AB + 0.84AC + 0.34AD - 1.98CD - 0.88B^2 - 1.34C^2 - 1.60D^2 \quad (29)$$

The good fit of the model equation was validated using the R^2 (coefficient of regression) method. The high coefficient of regression value of 0.9517 implied that 95.17 percent of the variability in the response can be explained by the model.

RSM plots

The RSM predicted against the actual plot (given in fig. S5 of the Supplementary Material) showed that the data points were closely assembled to the straight line. This lent credence to the high coefficient of regression of 0.9517, which implied a good correlation between the actual and

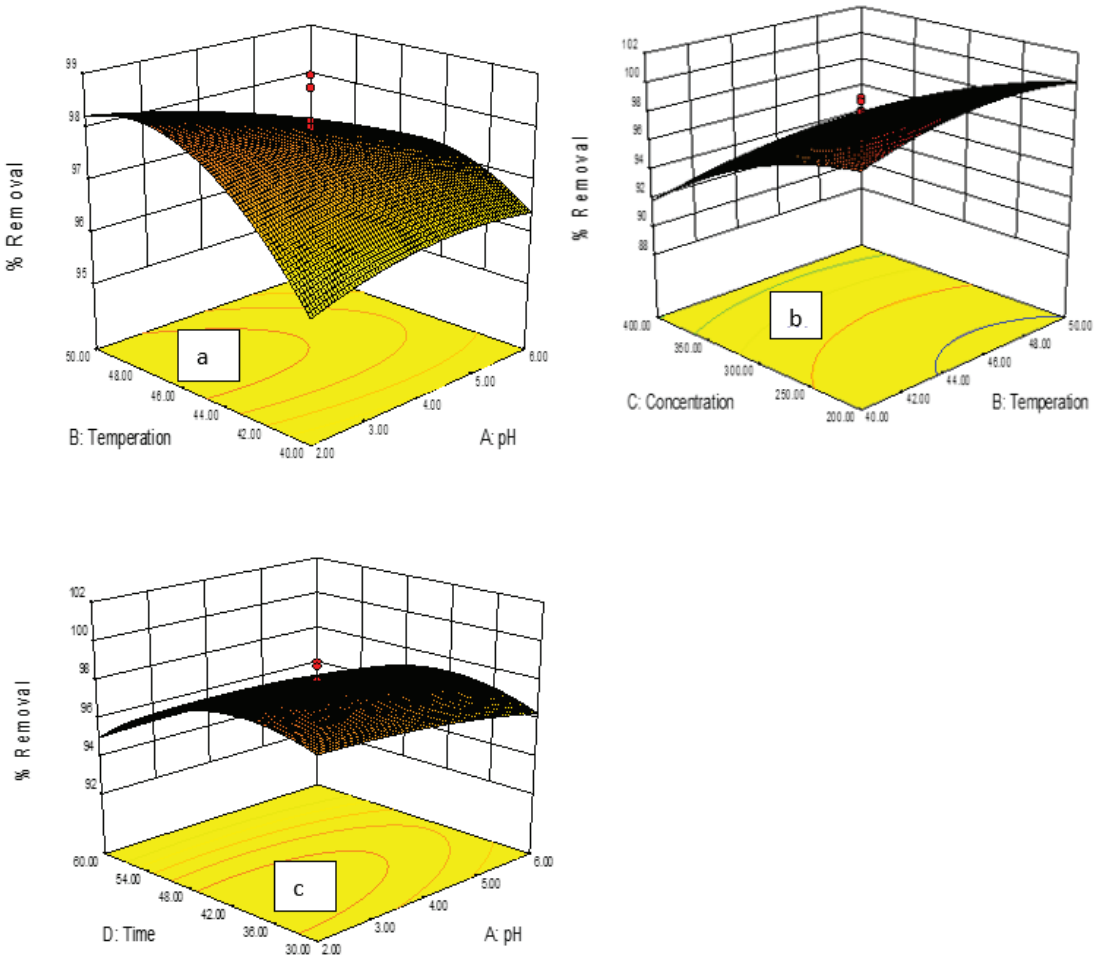

Figure 7. 3D surface plot for CR adsorption on the adsorbent showing combined effects of (a) pH and Temperature, (b) Temperature and Concentration, and (c) Temperature and Time.

predicted values of the response. The high R^2 confirmed that the quadratic model suggested was appropriate in describing the adsorption of the dye from an aqueous solution [93, 94]. Furthermore, a high R^2 of about 0.9517 indicates that the quadratic model generated was adequate in giving a significant prediction of the response within the studied range [40]. This phenomenon authenticated the assumptions of the above analysis.

The RSM 3D surface plots show the response surface measurements or the effect of any two independent process variables on the removal of CR. It usually depicts the graphical nature of the synergetic relationship between any two combined experimental variables and the response. Figures 7a-c, revealed the relationship between every two independent process variables. The spherical contours, as seen from the graphs, show a mutual significance between every two variables.

ANN Modeling

The artificial neural network for the adsorption of CR was modeled using the neural toolbox of MATLAB software. The best ANN with input, hidden, and output nodes of 4, 9, and 1 was used to model the optimum percentage removal of CR in the adsorption process. The input nodes represent the independent variables, while the output node represents the response, and the hidden layer reveals the nonlinear transformations on the input space. The optimal number of neurons in the hidden layer was determined by varying the number of neurons in the hidden layer and comparing the mean square error obtained. Therefore, the ANN topology architecture of 4-9-1, corresponding to the four input variables (temperature, pH, concentration, and contact time), nine neurons in the hidden layer, and one output variable (percentage adsorbed), was used in the ANN modeling. Levenberg-Marquardt (LM) back propagation was the algorithm utilized in the ANN modeling. Properties of the ANN model is given in Table 4.

Table 4. Properties of the ANN model

Algorithm	Back propagation
Error function	Mean square error
Input layer neuron	4
Hidden layer neuron	9
Output layer neuron	1
Training	Levenberg-Maraquardt
Hidden layer	Trainlm
Data division	Dividerand

The ANN validation plot (given in Fig. S6 of the Supplementary Material) was used to describe the

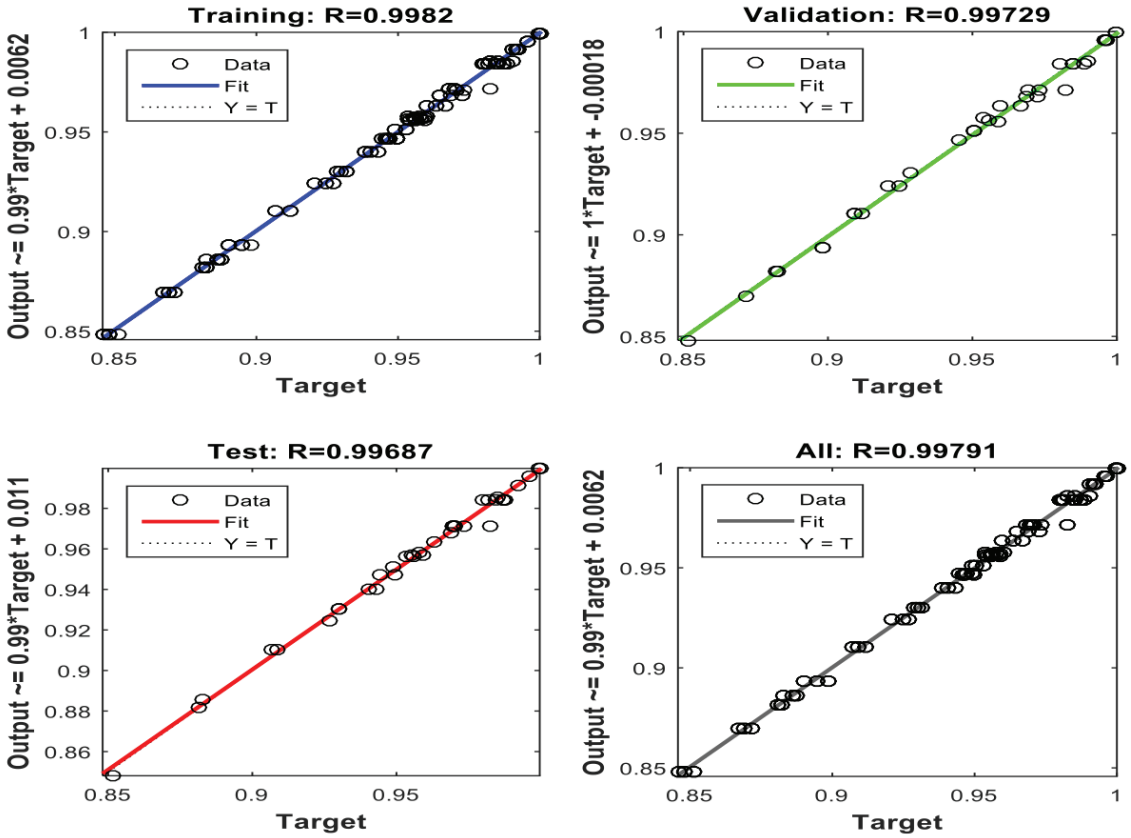

Figure 8. ANN regression plots for (A) training, (B) validation, (C) validation and (D) overall process.

Table 5. Properties of the ANFIS model

Number of inputs	4
Number of membership functions for each input	3
Number of data set	246
Number of output	1
Number of epochs	40
Output membership function	Constant
Input membership function	Gauss2mf
Method of optimization	Hybrid

validation of the neural network process at the 9th epoch iteration. The lowest mean square error of 9.56x10^{-6} was observed at the 6th epoch in Figure 12. This suggested that the MSE was minimal, indicating that the neural training was reliable with no over-fitting.

The experimental data sets were divided into training, validation, and testing so that there was no over-parameterization. Scatter diagrams that compared experimental data (target) with the computed neural data for training, validation, testing, and overall data are shown in Figure 8. The regression values of 0.9982, 0.9973, 0.9969, and 0.9979 were obtained for the training, validation, testing, and overall data, respectively. These values explain the satisfactory nature of the neural fittings. Besides, the outputs were very close to the targets, as most of the data points were aligned to the 45-degree line. The ANN predicted percentage of CR removal was presented in Table S3 of the supplementary material.

ANFIS Modeling

The ANFIS prediction technique was used to predict the percentage of CR dye adsorption using four input parameters: contact time, concentration, pH, and temperature. The ANFIS Sugeno diagram was displayed in Figure 9, and Table 5 listed the ANFIS features.

The ANFIS matrix involved 246x4 matrix (representing the input variables) and 246x1 matrix (representing the output variable) that were used in the MATLAB m-file. Gaussian combination membership function (Guass2mf) was employed in checking the grid partition. Three membership functions were assigned to each input layer in generating the FIS.

The ANFIS data was trained at 40 epoch iterations with an error tolerance of zero. A minimum error of 0.0025426 was produced after the 6th epoch, which lent credence to the adequacy of the ANFIS in modeling the adsorptive removal of CR dye. The plot of FIS against training data can be assessed in Fig. S7 of the Supplementary Material. A Hybrid-learning algorithm that makes use of the gradient method and the least square method was used in optimizing the ANFIS model. The correlation coefficient of 0.996 confirms the suitability of the ANFIS model in predicting the removal of CR from wastewater using Ihiala clay.

Models' Comparative Analysis

The predictive abilities of the ANFIS, ANN, and RSM models were compared in order to develop an ordered ranking. The experimental result, the models' predicted results, and the residual of the three models were compared and can be assessed in Table S3 of the Supplementary Material. The result showed that the three models were efficient in modeling and predicting the removal of CR from wastewater in an adsorption process. ANFIS with the lowest residuals in most experimental data sets seems to be the best at predicting the percentage of CR removed. Further statistical analyses were used to compare the adequacy of the three models in Table 6. The model parameters investigated include R^2, ARE, HYBRID, RMSE, and SSE. In all the model indices, RSM showed the least modeling and predictive ability. ANFIS exhibited the best predictive

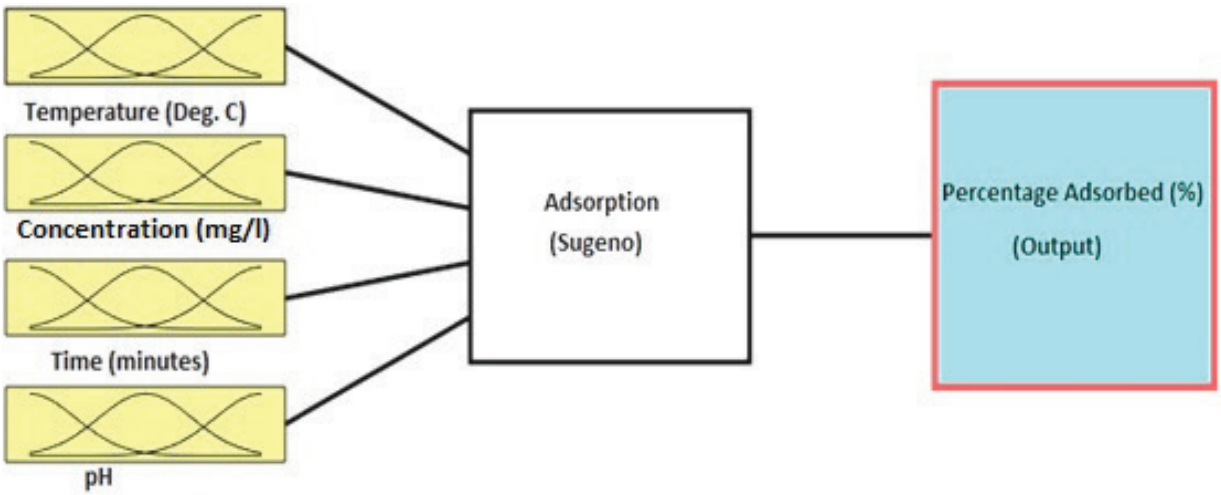

Figure 9. ANFIS Sugeno diagram of CR adsorption process.

Table 6. Comparative statistical analysis of RSM, ANN, and ANFIS models

Error function	Equation	RSM	ANN	ANFIS
Correlation coefficient	$R^2 = 1 - \frac{\sum_{i=1}^{n}(Y_{i,pre} - Y_{i,exp})^2}{\sum_{i=1}^{n}(Y_{i,exp} - Y_m)^2}$	0.9500	0.9958	0.9960
Average relative error	$ARE(\%) = \frac{100}{N}\sum_{i-1}^{N}\frac{\lvert P_{R,i,exp} - P_{R,i,cal}\rvert}{P_{R,i,exp}}$	0.7836	0.2090	0.2071
Sum of squared error	$\mathrm{SSE} = \sum_{i=1}^{n}\left(q_{e,cal} - q_{e,exp}\right)^2$	0.8764	0.0755	0.0712
Root mean square error	$RMSE = \sqrt{\frac{1}{N}\sum_{i=1}^{N}\left(\frac{P_{R,exp\,(i)} - P_{R,cal(i)}}{P_{R,exp\,(i)}}\right)^2}$	0.0094	0.0028	0.0027
Hybrid fractional error function	$HYBRID(\%) = \frac{1}{N-P}\sum\left[\frac{\left(P_{R,i,exp} - P_{R,i,cal}\right)^2}{P_{R,iexp}}\right]100$	0.8764	0.0755	0.0712

power when compared with the experimental data. It was closely followed by ANN. Therefore, it was concluded that ANFIS has the best generalization capacity regarding CR dye removal from wastewater. Onu et al. (2021), reported that ANFIS gave better prediction than ANN and RSM in the removal of eriochrome black-T dye [95].

Comparative Performance of the Adsorbent

A comparison of the adsorption of Congo red dye with other adsorbents was made to ascertain the efficiency and relevancy of the modified clay used in this study. Maximum adsorption capacity (q_{max}) and removal efficiency were the parameters utilized in the comparison, as shown in Table 7.

Table 7. Performance evaluation of different clay adsorbents based on removal efficiency and adsorption capacity of the clays in removal of organic pollutants from sewage

Adsorbent	Adsorb dos (g)	Removal eff (%)	Ads capacity (mg/g)	Reference
Composite clay	1	99.9	1649.3	[73]
Natural clay	2	93.8	88.86	[96]
Organo clay (H-Bt)	1.5	99	114.3	[38]
Organo clay (B-Bt)	1.5	67	165.56	[38]
Treated clay	0.3	90	39.80	[97]
Cu-pillar clay	1	99.9	222.22	[98]
Montomorillonite	1.5	99.5	122.09	[71]
Bentonite clay	1.5	94.7	161.3	[99]
Fe-bent	2	99	10.06	[70]
Bentonite composite	1.5	98.7	178.6	[100]
Pillared bentonite	2	89	121.3	[101]
Bentonite/GO	0.02	98	558.36	[101]
Modified clay (PCH)	0.025	70	28	[102]
Clay	0.25	85	67.11	[103]
Pillared clay (CrPC)	-	-	37.54	[104]
Pillared clay (AlPC)	-	-	24.33	
Modified red clay (MRC)	0.1	85	181.818	[105]
formulated clay-lime (F13 and F23)	0.1	82	7.87	[106]
Modified zeolite	0.05	79	114.989	[107]
Natural clay	0.25	99.17	74.35	[108]
Moroccan Clay	0.6	90	204	[109]
Modified clay	1	99.3	127.24	present study

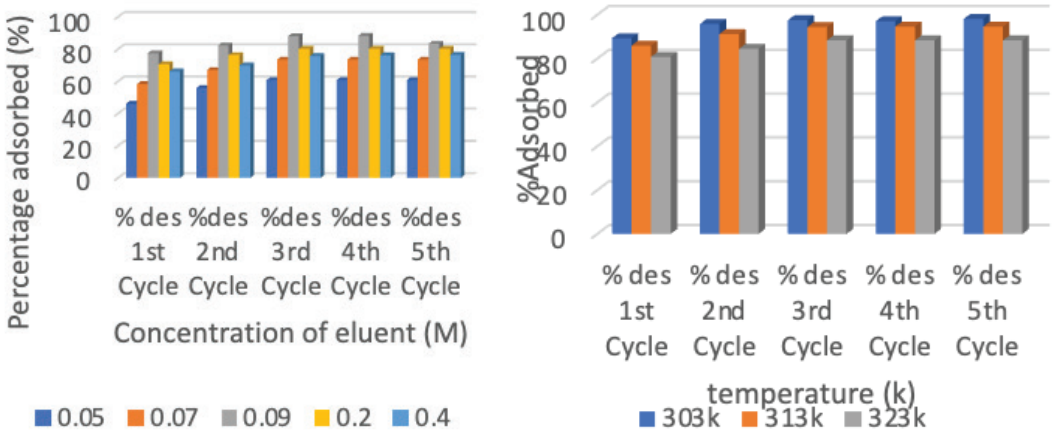

Figure 10. Effect of concentration of eluent and temperature on desorption of CR on PIC.

It is obvious from the table that the adsorption capacity of the modified Ihiala clay was higher than that of some other adsorbents. Besides, Ihiala clay is readily available as a large clay deposit in Ihiala town, Nigeria. This indicates that the abundant PIC, which is readily available with a relatively cost-effective method of activation, could be utilized as an effective and alternative adsorbent in the removal of Congo red dye from contaminated water.

Regeneration of Adsorbent

The effects of three different process variables were examined: concentration, pH, and temperature of the eluent. From the results of Figure 10, it is observed that the highest desorption percentages of 88.1, 91.5, and 97.5 % were achieved at an eluent (HCl) concentration of 0.09 mol, pH 5, and temperature of 303 k for a specific time of 150 minutes, while the highest desorption percentage of 95.7 was achieved using acetone at 303 k at the same time frame. After five successive desorption cycles, the high percentage of desorption at 0.09 concentration of eluent was due to HCl concentrations above 0.09 mole appearing to destabilize or damage the exhausted adsorbent structure, whereas slow desorption rates at lower concentrations were due to a weak driving force and thus required a larger volume of eluent to achieve the same objective as with higher concentrated eluent. Secondly, pH plays a vital role in the desorption process because desorption is simply the breaking of intermolecular bonds (van der Waals forces) that leads to adsorption via the exchange of ions between the eluent and saturated adsorbent. Furthermore, among the five cycles performed, the best-regenerated adsorbent was obtained at the fifth cycle. This was achieved after subjecting spent adsorbent or regenerated adsorbent at the end of each cycle to a fresh adsorption process. Finally, Fig. 10 also shows a nonsignificant change between the 3rd, 4th, and 5th desorption cycles, irrespective of whether the 5th has been the best. This minor change indicates that the process has attained equilibrium. A similar phenomenon was reported on the adsorption and desorption properties of polyethylenimine/polyvinyl chloride cross-linked fiber for the treatment of azo dye-reactive yellow 2 [110].

CONCLUSION

The present study established PIC as a reliable and quality adsorbent for dye uptake from an aqueous solution due to its high percentage adsorption and desorption capacities. The uptake of CR onto PIC was found to depend on the following factors: temperature, initial dye concentration, pH of solution, adsorbent particle size, contact time, and adsorbent dosage. The equilibrium adsorption data was best fitted by the Langmuir isotherm model, while the adsorption kinetics are best represented by pseudo-second-order kinetic models. The Langmuir model gave the highest maximum adsorption capacity (q_m) value of 127.24 mg g^{-1}. The ANN, ANFIS, and RSM models were found adequate in predictive modeling of the adsorption process, and the statistical analysis indicated that the ANFIS was marginally better than the ANN and RSM.

NOMENCLATURE

q	Adsorption capacity, mg g^{-1}.
q_e	Adsorption capacity at equilibrium, mg g^{-1}.
q_t	Adsorption capacity at time, mg g^{-1}.
K_L	Langmuir constants, L mg^{-1}.
R_L	Dimensional separation factor
K_f	Freundlich constants, L g^{-1}.
n	Freundlich constants
D	Effective diffusion coefficient, m^{2}s^{-1}.
R	Universal gas constants, J mol^{-1} K
PIC	Phosphoric acid Ihiala activated clay
T	Temperature, ^{o}C, K
q_D	Dubinin-Radushkevich constant, mg g^{-1}.
β	Constant related to sorption energy, mol^2
E	Mean free energy, KJ mol^{-1}.

C_o Initial concentration, mg L^{-1}.
K_2 Pseudo second-order kinetic constant
Kn Pseudo nth order kinetic constant
C_s Equilibrium concentration of dye on adsorbent, mg L^{-1}
C_e Equilibrium concentration of dye in solution, mg L^{-1}
K_d Intra-particle diffusion rate constant, mg $g^{-1}min^{1/2}$
ΔH Free enthalpy change, KJ mol^{-1}
ΔS Free entropy change, J mol^{-1} K
ΔG Free energy change, KJ mol^{-1}.
E_a Activation energy, KJ mol^{-1}.
q_m Maximum adsorption capacity
M Total mass of the adsorbent, g
W Weight of adsorbent
Δq_e Normalized standard deviation
HCl Hydrochloric acid
CR Congo red
A Elovich constants
nth Order of reaction
t Time (min)
C_t Concentration at time t, mg L^{-1}.
K_1 Pseudo first order kinetic constant
Kc Equilibrium constant

ACKNOWLEDGEMENT

The authors wish to appreciate Mr. Emmanuel Okafor of English department of St. John School Awka for proof-reading the manuscript.

AUTHORSHIP CONTRIBUTIONS

Authors equally contributed to this work.

DATA AVAILABILITY STATEMENT

The authors confirm that the data that supports the findings of this study are available within the article. Raw data that support the finding of this study are available from the corresponding author, upon reasonable request.

CONFLICT OF INTEREST

The author declared no potential conflicts of interest with respect to the research, authorship, and/or publication of this article.

ETHICS

There are no ethical issues with the publication of this manuscript.

REFERENCES

[1] Noroozi B, Soria GA, Bahrami IH, Arami M. Equilibrium and kinetic adsorption study of a cationic dye by natural adsorbent-silkworm pupa. J Hazard Mater 2007;139:167–174. [CrossRef]

[2] Abbasi MN, Asl R. Sonochemical degradation of basic blue 41 dye assisted by nano TiO_2 and H_2O_2. J Hazard Mater 2008;153:942–947. [CrossRef]

[3] Gupta VK, Jain R, Varshney S. Electrochemical removal of the hazardous dye Reactofix Red 3 BFN from industrial effluents. J Colloid Interface Sci 2007;312:292–296. [CrossRef]

[4] Sohrabi MR, Ghavami M. Photocatalytic degradation of Direct Red 23 dye using UV/TiO_2: Effect of operational parameters. J Hazard Mater 2008;153:1235–1239. [CrossRef]

[5] Daneshvar N, Khataee AR, Rasoulifard MH, Pourhassan M. Biodegradation of dye solution containing Malachite Green: Optimization of effective parameters using Taguchi method. J Hazard Mater 2007;143:214–219. [CrossRef]

[6] Fan L, Zhou Y, Yang W, Chen G, Yang F. Electrochemical degradation of aqueous solution of Amaranth azo dye on ACF under potentiostatic model. Dyes Pigments 2008;76:440–446. [CrossRef]

[7] Zonoozi MH, Moghaddam MRA, Arami M. Coagulation/flocculation of dye-containing solutions using polyaluminum chloride and alum. Water Sci Technol 2009;59:1343–1351. [CrossRef]

[8] Sachdeva S, Kumar A. Preparation of nonporous composite carbon membrane for separation of Rhodamine B dye. J Membr Sci 2009;329:2–10. [CrossRef]

[9] Tan LAW, Ahmad AL, Hameed BH. Adsorption of basic dye on high-surface-area activated carbon prepared from coconut husk: Equilibrium, kinetic and thermodynamic studies. J Hazard Mater 2008;154:337–346. [CrossRef]

[10] Gupta VK, Mittal A, Jain R, Mathur M, Sikarwar S. Photochemical degradation of hazardous dye Safranin-T using TiO_2 catalyst. J Colloid Interface Sci 2007;309:460–465. [CrossRef]

[11] Malik PK, Saha SK. Oxidation of direct dyes with hydrogen peroxide using ferrous ion as catalyst. Sep Purif Technol 2003;31:241–250. [CrossRef]

[12] Lorenc-Grabowska E, Gryglewicz G. Adsorption characteristics of Congo Red on coal-based mesoporous activated carbon. Dyes Pigments 2007;74:34–40. [CrossRef]

[13] Onukwuli OD, Oguanobi NC. Equilibrium, kinetic and thermodynamic adsorption study of cationic dye from aqueous solution onto modified Awka clay. IJNR Eng Sci 2017;4:1–16.

[14] Onu CE, Nwabanne JT. Application of response surface methodology in Malachite Green adsorption using Nteje clay. Open J Chem Eng Sci 2014;1:19–33.

[15] Akande JA, Adeogun AI, Uzosike AS. Removal of Congo Red dye from simulated wastewater using activated carbon derived from corn cobs; kinetics and equilibrium studies. Glob J Pure Appl Chem Res 2023;11:1–19. [CrossRef]

[16] Tabak A, Eren E, Afsin B, Caglar B. Determination of adsorptive properties of a Turkish sepiolite for removal of Reactive Blue 15 anionic dye from aqueous solutions. J Hazard Mater 2009;161:1087–1094. [CrossRef]
[17] Akar ST, Recep U. Untreated clay with high adsorption capacity for effective removal of C.I. Acid Red 88 from aqueous solutions: Batch and dynamic flow mode studies. J Chem Eng 2010;162:591–598. [CrossRef]
[18] Mohammed GH, Magdy AW, Hosni AG, Ahmed SE. Adsorption of Rose Bengal dye from wastewater onto modified biomass. Sci Rep 2023;13:14776. [CrossRef]
[19] Zhi L, Xiaohai H, Yi M, Bing G, Yiling S, Jianghui Z, Soon HT. Eggplant biomass-based porous carbon for fast and efficient dye adsorption from wastewater. Ind Crops Prod 2022;187:115510. [CrossRef]
[20] Dal SK, Meenal G. Treatment of textile dyeing effluent using agriculture waste-based adsorbents: A review. Chem Sci Int J 2022;32.
[21] Bhattacharyya KG, Sharma A. Kinetics and thermodynamics of Methylene Blue adsorption on Neem (Azadirachta indica) leaf powder. Dyes Pigments 2005;65:51–59. [CrossRef]
[22] Arana JMRR, Mazzoco RR. Adsorption studies of Methylene Blue and phenol onto black stone cherries prepared by chemical activation. J Hazard Mater 2010;180:656–661. [CrossRef]
[23] Doğan M, Abak H, Alkan M. Adsorption of Methylene Blue onto hazelnut shell: Kinetics, mechanism and activation parameters. J Hazard Mater 2009;164:172–181. [CrossRef]
[24] El-Halwany MM. Study of adsorption isotherms and kinetic models for Methylene Blue adsorption on activated carbon developed from Egyptian rice hull (Part II). Desalination 2010;250:208–213. [CrossRef]
[25] Hameed BH, Ahmad AL, Latiff KNA. Adsorption of basic dye (Methylene Blue) onto activated carbon prepared from rattan sawdust. Dyes Pigments 2007;75:143–149. [CrossRef]
[26] Hameed BH, Ahmad AL. Batch adsorption of Methylene Blue from aqueous solution by garlic peel, an agricultural waste biomass. J Hazard Mater 2009;164:870–875. [CrossRef]
[27] Xue SW, Jing PC. Biosorption of Congo Red from aqueous solution using wheat bran and rice bran: Batch studies. Sep Sci Technol 2009;44:1452–1466. [CrossRef]
[28] Hameed BH. Removal of cationic dye from aqueous solution using Jackfruit peel as non-conventional low-cost adsorbent. J Hazard Mater 2009;162:344–350. [CrossRef]
[29] Jaikumar V, Shathish Kumar K, GnanaPrakash D. Biosorption of acid dyes using spent brewery grains: Characterization and modeling. Int J Appl Sci Eng 2009;7:115–125.
[30] Hameed BH, El-Khaiary MI. Sorption kinetics and isotherm studies of a cationic dye using agricultural waste: Broad bean peels. J Hazard Mater 2008;154:639–648. [CrossRef]
[31] Vimonses V, Lei S, Jin B, Chow CWK, Saint C. Kinetic study and equilibrium isotherm analysis of Congo Red adsorption by clay materials. J Chem Eng 2009;148:354–364. [CrossRef]
[32] Onu CE, Oguanobi NC, Okonkwo CO, Nnamdi-Bejie J. Application of modified agricultural waste in the adsorption of Bromocresol Green dye. Asian J Chem Sci 2020;7:15–24. [CrossRef]
[33] Juraj B. Controversial issues related to dye adsorption on clay minerals: A critical review. Molecules 2023;28:6951. [CrossRef]
[34] El Kerdoudi Z, Bensalah J, Ferraa N, El Mekkaoui A, Berisha A, Safi Z, et al. Physicochemical characterization of clay and study of cationic Methylene Blue dye adsorption. ACS Omega 2023;8:40848–40863. [CrossRef]
[35] Mohammed B, Mustapha D, Ftiha D. Adsorption of dye using natural clay from water. J Environ Eng Sci 2022;17:175–183. [CrossRef]
[36] Muhammed O, Çiğdem SÖ. Equilibrium studies for dye adsorption onto red clay. MTU J Eng Nat Sci 2022;3:36–45.
[37] Sabarish R, Jasila K, Aswathy J, Jyotishkumar P, Jaewoo L, Jyothi Mannekote S, et al. Adsorption of anionic dye onto ZSM-5 zeolite-based bio membrane: Characterizations, kinetics and adsorption isotherm. J Polym Environ 2022. Preprint. Doi: 10.21203/rs.3.rs-1191111/v1 [CrossRef]
[38] Nayoon C, Yeongkyun S, Tae-Hyun K, Yuri P, Yuhoon H. Adsorption behaviors of modified clays prepared with structurally different surfactants for anionic dyes removal. Environ Eng Res 2023;28:210076.
[39] McKay G. The adsorption of dyestuffs from aqueous solutions using activated carbon: External mass transfer processes. J Chem Technol Biotechnol 1983;33A:205–218. [CrossRef]
[40] Oguanobi NC, Onu CE, Onukwuli OD. Adsorption of a dye (Crystal Violet) on acid-modified non-conventional adsorbent. J Chem Technol Metall 2019;54:95–110.
[41] Nwobasi VN, Igbokwe PK, Onu CE. Removal of Methylene Blue dye from aqueous solution using modified Ngbo clay. J Mater Sci Res Rev 2020;5:33–46.
[42] Tsai WT, Chang CY, Lin MC, Chien SF, Sun HF, Hsieh MF. Adsorption of acid dye onto activated carbons prepared from agricultural waste bagasse by $ZnCl_2$ activation. Chemosphere 2001;45:51–58. [CrossRef]
[43] Mahammedi F, Benguella B. Adsorption of Methylene Blue from aqueous solutions using natural clay. J Mater Environ Sci 2016;7:285–292.

[44] Venkatesh PM, Karthikeyan R. Comparative studies on modeling and optimization of hydrodynamic parameters on inverse fluidized bed reactor using ANN-GA and RSM. Alexandria Eng J 2018;57:3019–3032. [CrossRef]

[45] Onu CE, Igbokwe PK, Nwabanne JT, Nwanjinka OC, Ohale PE. Evaluation of optimization techniques in predicting optimum moisture content reduction in drying potato slices. Artif Intell Agric 2020;4:39–47. [CrossRef]

[46] Betiku E, Osunleke AS, Odude VO, Bamimore A, Oladipo B, Okeleye AA, et al. Performance evaluation of adaptive neuro-fuzzy inference system, artificial neural network and response surface methodology in modeling biodiesel synthesis from palm kernel oil by transesterification. Biofuels 2018;1–17. [CrossRef]

[47] Gonzalez CRT, Subathra MSP, Manoj NKN. Modeling the daily reference evapotranspiration in semi-arid region of South India: A case study comparing ANFIS and empirical models. Inf Process Agric 2020;2–12.

[48] Najafi B, Faizollahzadeh Ardabili S. Application of ANFIS, ANN, and logistic methods in estimating biogas production from spent mushroom compost (SMC). Resour Conserv Recycl 2018;133:169–178. [CrossRef]

[49] Langmuir I. The constitution and fundamental properties of solids and liquids. J Am Chem Soc 1916;38:2221–2295. [CrossRef]

[50] Freundlich H. Over the adsorption in solution. J Phys Chem 1906;57:385–470. [CrossRef]

[51] Vieth WR, Sladek KJ. A model for diffusion in a glassy polymer. J Colloid Sci 1965;20:1014–1033. [CrossRef]

[52] Dubinin MM, Radushkevich LV. Equation of the characteristic curve of activated charcoal. Proc Acad Sci Phys Chem Sect USSR 1947;55:331–333.

[53] Elovich SY, Larinov OG. Theory of adsorption from solutions of non-electrolytes on solid: (I) Equation adsorption from solutions and the analysis of its simplest form, (II) Verification of the equation of adsorption isotherm from solutions. Izv Akad Nauk SSSR Otd Khim Nauk 1962;2:209–216. [CrossRef]

[54] Lagergren S. Zur theorie der sogenannten adsorption geloster stoffe. Kungl Sven Vetenskapsakad Handl 1898;24:1–39.

[55] Ritchie AG. Alternative to the Elovich equation for the kinetics of adsorption of gases on solids. J Chem Soc Faraday Trans 1 Phys Chem Condens Phases 1977;73:1650–1653. [CrossRef]

[56] Ho YS, Wase DAJ, Forster CF. Removal of lead ions from aqueous solution using sphagnum moss peat as adsorbent. Water SA 1996;22:219–224.

[57] Ho YS, McKay G. Pseudo second-order model for sorption process. Process Biochem 1999;34:451–465. [CrossRef]

[58] Weber WJ, Morris JC. Kinetics of adsorption on carbon from solutions. J Sanit Eng Div 1963;89:31–39. [CrossRef]

[59] Spahn H, Schlunder U. The scale-up of activated carbon columns for water purification based on results from batch tests. I. Theoretical and experimental determination of adsorption rates of single organic solutes in batch tests. Chem Eng Sci 1975;30:529–537. [CrossRef]

[60] Boyd GE, Adamson AW, Meyers LS Jr. The exchange adsorption of ions from aqueous solutions by organite-zeolites. II. Kinetics. J Am Chem Soc 1947;69:2836. [CrossRef]

[61] Nwabanne JT, Okpe EC, Asadu CO, Onu CE. Sorption studies of dyestuffs on low-cost adsorbent. Asian J Phys Chem Sci 2018;5:1–19. [CrossRef]

[62] Arulkumar M, Sathishkumar P, Palvannan T. Optimization of Orange G dye adsorption by activated carbon of Thespesia populnea pods using response surface methodology. J Hazard Mater 2011;186:827–834. [CrossRef]

[63] Manpreet SB, DhritiKapoor RK, Kalia ASR, Ashwani KT. RSM and ANN modeling for electrocoagulation of copper from simulated wastewater: Multiobjective optimization using genetic algorithm approach. Desalination 2011;274:74–80. [CrossRef]

[64] Mingyi F, Tongjun L, Jiwei H, Rensheng C, Xionghui W, Xuedan S, et al. Artificial neural network modeling and genetic algorithm optimization for cadmium removal from aqueous solutions by reduced graphene oxide-supported nanoscale zero-valent iron (nZVI/rGO) composites. Materials (Basel) 2017;10:1–22. [CrossRef]

[65] Mourabet ME, Rhilassi A, Bennani-Ziatni M, Taitai A. Comparative study of artificial neural network and response surface methodology for modeling and optimization of the adsorption capacity of fluoride onto apatitic tricalcium phosphate. Univ J Appl Math 2014;2:84–91. [CrossRef]

[66] Bahman N, Sina FA. Application of ANFIS, ANN, and logistic methods in estimating biogas production from spent mushroom compost (SMC). Resour Conserv Recycl 2018;133:169–178. [CrossRef]

[67] Wu X, Hui KN, Lee SK, Zhou W, Chen R, Hwang DH, et al. Adsorption of Basic Yellow 87 from aqueous solution onto two different mesoporous adsorbents. Chem Eng J 2012;180:91–98. [CrossRef]

[68] Ladhe UV, Wankhede SK, Patil VT, Patil PR. Adsorption of Eriochrome Black-T from aqueous solution on activated carbon prepared from Mosambi peel. J Appl Sci Environ Sanit 2011;6:149–154.

[69] Ismat AE, Marufa K, Most Afroza K, Owaleur RM, Anis-Ul-Haque KM, Jegede MM, et al. Sequestration of hazardous dyes from aqueous solution using raw and modified agricultural waste. Adsorpt Sci Technol 2021;2021:6297451. [CrossRef]

[70] Barakan S, Aghazadeh V, Samiee BA, Mohammadi S. Thermodynamic, kinetic, and equilibrium isotherm studies of As(V) adsorption by Fe(III)-impregnated bentonite. Environ Dev Sustain 2020;22:5273–5295. [CrossRef]

[71] Mahmoud EO, Mohamed L, Hicham AO, Younes B, Abdelhadi A, Abdelaziz E, et al. Efficient removal of p-nitrophenol from water using montmorillonite clay: Insights into the adsorption mechanism, process optimization, and regeneration. Environ Sci Pollut Res 2019;26:19615–19631. [CrossRef]

[72] Imessaoudene A, Cheikh S, Hadadi A, Hamri N, Bollinger JC, Amrane A, et al. Adsorption performance of zeolite for the removal of Congo Red dye: Factorial design experiments, kinetic, and equilibrium studies. Separations. 2023;10:57. [CrossRef]

[73] Adebayo MA, Jabar JM, Amoko JS, Openiyi EO, Shodiya OO. Coconut husk-raw clay-Fe composite: Preparation, characteristics, and mechanisms of Congo Red adsorption. Sci Rep 2022;12:14370. [CrossRef]

[74] Reddy SMC, Sivaramakrishna L, Reddy VA. The use of an agricultural waste material, Jujba seeds, for the removal of anionic dye (Congo Red) from aqueous medium. J Hazard Mater 2012;203–204:118–127. [CrossRef]

[75] Popoola TJ, Okoronkwo AE, Oluwasina OO, Adebayo MA. Preparation, characterization, and application of homemade graphene for the removal of Congo Red from aqueous solutions. Environ Sci Pollut Res 2021;28:52174–52187. [CrossRef]

[76] Lafi R, Montasser I, Hafiane A. Adsorption of Congo Red dye from aqueous solutions by prepared activated carbon with oxygen-containing functional groups and its regeneration. Adsorpt Sci Technol 2019;37:160–181. [CrossRef]

[77] Mahmoodi M, Hayati MB, Arami M, Lan C. Adsorption of textile dyes on pine cone from colored wastewater: Kinetic, equilibrium, and thermodynamic studies. Desalination 2011;268:117–125. [CrossRef]

[78] Salleh MAM, Mahmoud DK, Karim WA, Idris A. Cationic and anionic dye adsorption by agricultural solid waste: A comparative review. Desalination 2011;280:1–13. [CrossRef]

[79] Lata H, Garg V, Gupta R. Removal of basic dye from aqueous solution by adsorption using Parthenium hysterophorus: An agricultural waste. Dyes Pigments 2007;74:653–658. [CrossRef]

[80] Ho YS, Porter JF, McKay G. Equilibrium isotherm studies for the sorption of divalent metal ions onto peat: Copper, nickel, and lead single-component system. Water Air Soil Pollut 2002;141:1–33.

[81] Ho YS, Wase DAJ, Forster CF. Removal of lead ions from aqueous solution using sphagnum moss peat as adsorbent. Water SA 1996;22:219–224.

[82] Singha B, Das SK. Adsorptive removal of Cu(II) from aqueous solution and industrial effluent using natural and agricultural waste. Colloids Surf B 2013;107:77–106. [CrossRef]

[83] Kausar A, Bhatti H, Mackinnon G. Equilibrium kinetic and thermodynamics studies on the removal of U(VI) by low-cost agricultural waste. Colloids Surf B 2013;111:124–133. [CrossRef]

[84] Malash GF, El-Khaiary MI. Methylene Blue adsorption by the waste of Abu-Tartour phosphate rock. J Colloid Interface Sci 2010;348:537–545. [CrossRef]

[85] Srivastava VC, Mall ID, Mishra M. Adsorption thermodynamics and isosteric heat of adsorption of toxic metal ion onto bagasse fly ash (BFA) and rice husk ash (RHA). Chem Eng J 2007;132:267–278. [CrossRef]

[86] Cheung WH, Szeto YS, McKay G. Intraparticle diffusion processes during acid dye adsorption onto chitosan. Bioresour Technol 2007;98:2897–2904. [CrossRef]

[87] Cáceres-Jensen L, Rodríguez-Becerra J, Parra-Rivero J, Escudey M, Barrientos L, Castro-Castillo V. Sorption kinetics of Diuron on volcanic ash-derived soils. J Hazard Mater 2013;261:602–613. [CrossRef]

[88] Hu Z, Chen H, Ji F, Yuan S. Removal of Congo Red from aqueous solution by cattail root. J Hazard Mater 2010;173:292–297. [CrossRef]

[89] Dalia KM, Mohamad AMS, Wan AWAK, Azni I, Zurina ZA. Batch adsorption of basic dye using acid-treated kenaf fiber char: Equilibrium, kinetic, and thermodynamic studies. Chem Eng J 2011;181–182:449–457. [CrossRef]

[90] Wu CH. Adsorption of reactive dye onto carbon nanotubes: Equilibrium, kinetics, and thermodynamics. J Hazard Mater 2007;144:93–100. [CrossRef]

[91] Amini A, Younesi H, Bahramifar N, Lorestani A, Ghorbani F, Daneshi A, Sharifzadeh M. Application of response surface methodology for optimization of lead biosorption in an aqueous solution by Aspergillus niger. J Hazard Mater 2008;154:694–702. [CrossRef]

[92] Kim HK, Kim JG, Cho JD, Hong JW. Optimization and characterization of UV-curable adhesive for optical communication by response surface methodology. Polym Test 2003;22:899–906. [CrossRef]

[93] Onu CE, Nwabanne JT. Application of response surface methodology in Malachite Green adsorption using Nteje clay. Open J Chem Eng Sci 2014;1:19–33.

[94] Iheanacho CO, Nwabanne JT, Onu CE. Optimum process parameters for activated carbon production from rice husk for phenol adsorption. Curr J Appl Sci Technol 2019;36:1–11. [CrossRef]

[95] Onu CE, Nwabanne JT, Ohale PE, Asadu CO. Application of ANN and RSM techniques in optimal parameter evaluation for turbidity removal from abattoir effluent using valorized chicken bone coagulant. S Afr J Chem Eng 2021;36:24–42.

[96] Foroutan R, Mohammadi R, Adeleye AS, Farjadfad S, Esvandi Z, Arfaeinia H, et al. Efficient arsenic(V) removal from contaminated water using natural clay and clay composite adsorbents. Environ Sci Pollut Res 2019;26:29748–29762. [CrossRef]

[97] Paul ED, Mutsee T. Treated clay mineral as adsorbent for the removal of heavy metals from aqueous solution. Appl Sci Eng Prog 2021;14.

[98] Georgescu AM, Nardou F, Zichil V, Nistor ID. Adsorption of lead(II) ions from aqueous solutions onto Cr-pillared clays. Appl Clay Sci 2018;152:44–50. [CrossRef]

[99] Ahmadi A, Foroutan R, Esmaeili H, Tamjidi S. The role of bentonite clay and bentonite clay@$MnFe_2O_4$ composite and their physico-chemical properties on the removal of Cr(III) and Cr(VI) from aqueous media. Environ Sci Pollut Res 2020;27:14044–14057. [CrossRef]

[100] Chang YS, Au PI, Mubarak NM, Khalid M, Jagadish P, Walvekar R, Abdullah EC. Adsorption of Cu(II) and Ni(II) ions from wastewater onto bentonite and bentonite/GO composite. Environ Sci Pollut Res 2020;27:33270–33296. [CrossRef]

[101] Barakan S, Aghazadeh V. Structural modification of nano bentonite by aluminum, iron pillarization, and 3D growth of silica mesoporous framework for arsenic removal from gold mine wastewater. J Hazard Mater 2019;378:120779. [CrossRef]

[102] Darlyson TG, Liana MRM, Luiz BdSS, Edy SB, Enrique V, Enrique R, et al. Purification of anthocyanins (Brassica oleracea var. Rubra) from purple cabbage using natural and modified clays as adsorbent. Adsorpt Sci Technol 2023;2023:2724122. [CrossRef]

[103] Metin A, Ahmet G, Kübra G, Elif Ş. Adsorption of textile dyes from aqueous solutions onto clay: Kinetic modeling and equilibrium isotherm analysis. Front Chem 2023;11. [CrossRef]

[104] Hari D, Kannan A. Adsorption of organic dye on pillared clays. Proceedings of the 9th World Congress on New Technologies (NewTech'23). 2023;Paper No. ICEPR 138.

[105] Carazeanu PI, Roscaa I, Dumbravaa A. Modified red clays as adsorbents in the removal of cationic dyes from aqueous solutions. Dig J Nanomater Biostruct 2023;18:567–578. [CrossRef]

[106] Fumba G, Essomba JS, Ankoro NO, Kouotou D, Bélibi BPD, Ndi JN, Ketcha MJ. CI Acid Orange 52 dye removal using natural and formulated clay-lime materials: Isotherm, kinetic, and thermodynamic studies. J Mater Sci Chem Eng 2023;11. [CrossRef]

[107] Laura AP, Adrián B, María EG, Yenetzi V, Ana GC, María SB. Adsorption of arsenic, lead, cadmium, and chromium ions from aqueous solution using a protonated chabazite: Preparation, characterization, and removal mechanism. Adsorpt Sci Technol 2023;2023:2018121. [CrossRef]

[108] Fuad HSR, Dler MSS, Stephan K. Adsorption study and removal of Basic Fuchsin dye from medical laboratory wastewater using local natural clay. Adsorpt Sci Technol 2023;2023:9398167. [CrossRef]

[109] Abdelfattah EM, Yassine E, Souad Z, Issam M. Elaboration and characterization of Organo-Ghassoul (Moroccan clay) as an adsorbent using cationic surfactant for anionic dye adsorption. Phys Chem Res 2023;11:913c928.

[110] Wang G, He D, Fengchun ZF, Hu J, Lee Y, Shi J, Xu J. Extraction and purification of ustiloxin A from rice false smut balls by a combination of macroporous resin and high-speed countercurrent chromatography. Food Prod Process Nutr 2020;2:29. [CrossRef]